Rare Earth Metal Cluster Complexes

Gerd Meyer

Universität zu Köln, Köln, Germany

1 SUMMARY

The valence electron (VE) situation of the group 3 elements scandium, yttrium, lanthanum, and the following 14 ''4f elements'' cerium through lutetium is such that three electrons may be considered as the valence shell (s^2d^1), with the 4f electrons to be considered as core electrons. The latter often determine important properties (magnetism, absorption and emission of light) but their contribution to chemical bonding is negligible. With the paucity of three VEs, these elements may form (in the majority of cases octahedral) clusters, although almost always incorporating an endohedral atom (or atom group) that contributes to the overall electron count. For a general cluster complex $\{ZR_x\}X_z$, contributions to chemical bonding are mostly heteroatomic, of the Z–R and R–X type, with little homoatomic Z–Z and R–R contributions. Thus, these cluster complexes may be understood as anti-Werner-type complexes with the polarity of the atoms being textsf−(Z), +(R), −(X). In rare cases, the cluster complexes are isolated, or, more frequently, connected via common ligands. In the majority of cases, the clusters share common edges (or faces) to oligomers, chains, layers, or even networks.

2 INTRODUCTION

Clusters consist of two or more atoms of the same element bound together by considerable bonding interactions.[1] Clusters may be naked and neutral like $\{Au_{20}\}$ or charged as $\{Bi_9\}^{5+}$ and $\{Pb_5\}^{2-}$, respectively. Cluster complexes are clusters surrounded by ligands. Prominent examples are $[\{Mo_6\}Cl_{14}]^{2-}$ or $\{Rh_6\}(CO)_{16}$. These examples represent two types of transition metal cluster complexes. The first type consists of the rather electron-rich metal atom clusters surrounded by electronegative ligands without any ability for π back bonding. In the second type, the ligands are involved in distinct π back bonding, with the 18 valence-electron rule being typically obeyed.

In early transition metal clusters, 24- or 16-electron rules play an important role. In the salt $K_2[\{Mo_6\}Cl_{14}]$, there are 24 electrons available for intracluster bonding. In a valence bond (VB) interpretation, they build 12 equal two-center–two-electron (2 c–2e) bonds, locally associated with the edges of the octahedral $\{Mo_6\}$ cluster. In a molecular orbital (MO) theory description, 12 bonding MOs are occupied, with the LUMO already antibonding. In $K_4[\{Nb_6\}Cl_{18}]$, 16 cluster-based electrons occupy eight three-center–two-

The Rare Earth Elements. Edited by David A. Atwood. ISBN 978-1-119-95097-4

electron (3c–2e) bonds, according to the VB theory. Elements such as Zr (4 VE), with fewer VE than Mo (6 VE) or Nb (5 VE), may also form cluster complexes and obey, more or less, the 16-electron rule through incorporation of an endohedral atom in the center of the cluster as in $K_2Zr[\{CZr_6\}Cl_{18}]$, a single carbon atom in this case. Note that there are only nine cluster-based electrons—mostly for carbon–lutetium bonding interactions—in $Cs_2Lu[\{CLu_6\}Cl_{18}]$, although it has the same structure as the just mentioned zirconium compound.

The binary chloride $\{Nb_6\}Cl_{14}$ has the same number of cluster-based electrons, 16, as the ternary salt $K_4[\{Nb_6\}Cl_{18}]$, but fewer ligands to surround the cluster. Thus, the cluster complexes have to share ligands. In $\{Nb_6\}Cl_{14}$, this is accomplished in a rather complicated way, depicted as $\{Nb_6\}Cl_{10/1}{}^{i}Cl_{4/2}{}^{a-a}Cl_{2/2}{}^{i-a}Cl_{2/2}{}^{a-i}$, see Figure 1. The nomenclature used here is that of Niggli, Schäfer, and Schnering as well as that proposed recently by the author of this chapter; clusters with or without endohedral atoms are included in waved braces.[2–5] $\{CZr_6\}Cl_{14}$ has essentially the same structure, with a carbon atom in the center of the zirconium octahedron. The $\{CZr_6\}$ cluster is short of two electrons to obey the 16-electron rule. However, a view of the MO diagram calculated by extended Hueckel molecular orbital (EHMO) theory shows that the a_{2u} orbital, although bonding in character, is rather high in energy, see Figure 2. Quite obviously the cluster complex compound is stabilized by the formation of an extended salt through lattice energy contributions.

The rare earth elements (Sc, Y, and the lanthanides La–Lu) have only three VEs available for bonding in clusters, $ns^2(n-1)d^1(n-2)f^n$; f electrons, if present, do not engage in bonding. Therefore, clusters without an endohedral atom (''interstitial'') are extremely rare, although Gd_2Cl_3 with empty $\{Gd_6\}$ clusters was the first known example containing a

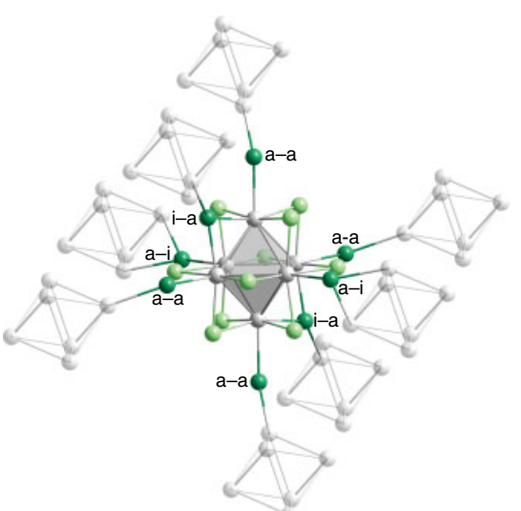

Figure 1 One cluster complex $\{Nb_6\}Cl_{12}{}^{i}Cl_6{}^{a}$ connected via a–a and i–a/a–i bridges to eight surrounding clusters (a stands for outer, German: äußere, i for inner(e) ligands

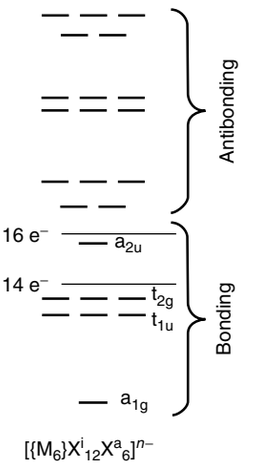

Figure 2 Schematic MO diagram for $[\{ZM_6\}X^{i}{}_{12}X^{a}{}_6]^{n-}$ cluster complexes

rare earth metal cluster, see Chapter 4 and Refs 19–22 therein. Isolated rare earth cluster complexes with interstitials such as $Cs_2Lu[\{CLu_6\}Cl_{18}]$ are also rare; more frequent are cluster complexes connected via common ligands, for example, $\{CSc_6\}I_{12}Sc$ (with a 13-electron cluster) or $\{IrPr_6\}Cl_{10}$ (with a 17-electron cluster). Most frequent are, however, compounds in which the clusters are connected via common edges (or faces). Examples are $\{(C_2)_2Dy_{10}\}Br_{18}$ (common edge of two $\{(C_2)Dy_6\}$ clusters in a dimer) or $\{OsSc_4\}Cl_4$ (two common opposite faces of square antiprisms, resulting in a chain).

Cluster complexes are not known for all rare earth elements. Bonding in the cluster $\{ZR_x\}$ is predominantly achieved by heteroatomic Z-R interactions with usually little homoatomic R-R contributions. Therefore, p states for main-group elements and d states for transition metal atoms as endohedral atoms Z have to match d states of the rare earth elements in energy and symmetry. In a localized view, the number of electrons has to be sufficient to occupy enough bonding orbitals. As almost all cluster complexes are structurally of the $[\{ZR_6\}X^{i}{}_{12}X^{a}{}_6]$ type, 16–18 electrons with an endohedral transition metal atom and 14 with a main-group atom are good rules of thumb. Figure 3 shows an EHMO calculation for $[\{IrY_6\}I_{18}]^{8-}$, a 17-electron cluster cut out of the extended solid $\{IrY_6\}I_{10}$; the SOMO still has bonding character and is separated from the LUMO by almost 4 eV.

Crystal orbital Hamiltonian population (COHP) diagrams derived from band structure calculations for the extended solid $\{IrY_6\}I_{10}$ show that Ir–Y and Y–I bonding interactions are most prominent, with considerable Ir–Y bonding and some Y–I antibonding interactions just below the Fermi level. Y-Y bonding plays only a negligible role, see Figure 4.

In a thermodynamic view, only those rare earth elements may form clusters for which the reduction to an alkaline-earth-like divalent state with no occupation of a

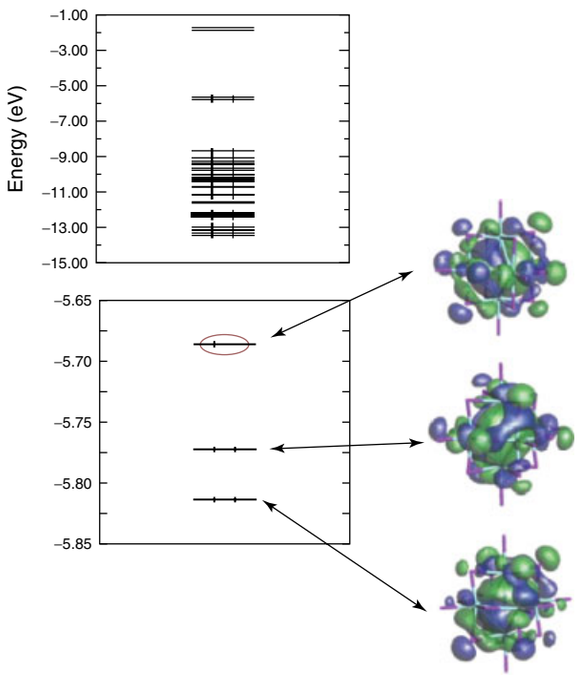

Figure 3 EHMO calculation for $[\{IrY_6\}I_{18}]^{8-}$, a 17-electron cluster cut out of the extended solid $\{IrY_6\}I_{10}$. The lower part shows two HOMOs and the SOMO

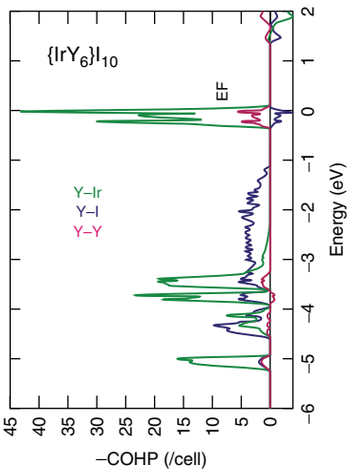

Figure 4 A crystal orbital Hamiltonian population (COHP) diagram for $\{IrY_6\}I_{10}$, derived from LMTO-ASA band structure calculations

5d state is not feasible. Important terms in an appropriate thermodynamic cycle are the lattice energies and atomic data as enthalpies of sublimation and of ionization. Most of these values parallel the lanthanide contraction and are aperiodic. However, the third ionization potentials show a periodic behavior throughout the lanthanide series, see Figure 5. For further information, see Refs 6–11.

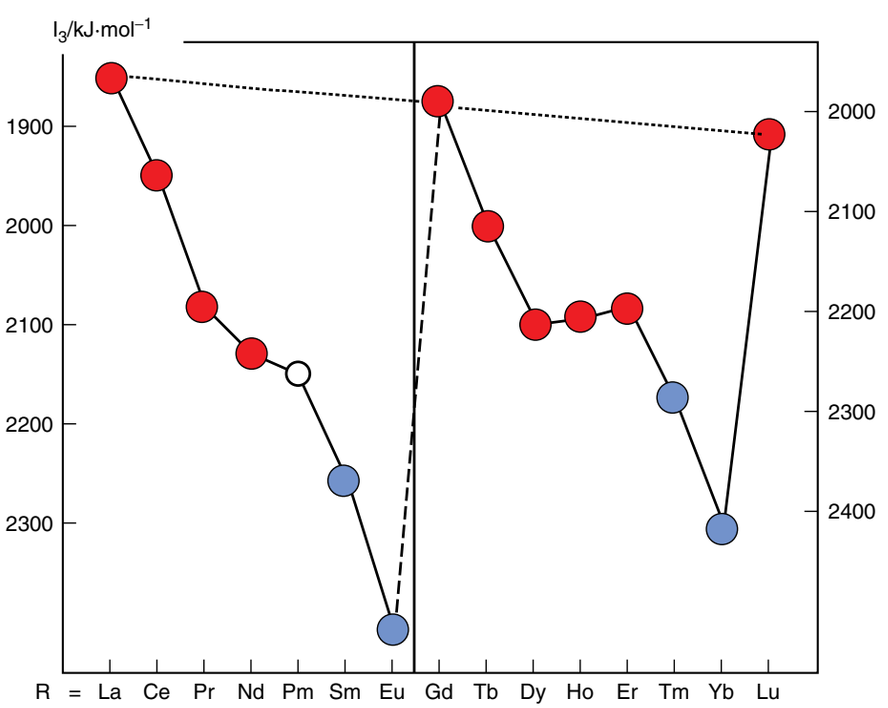

Figure 5 Third ionization potential I_3 versus atomic number for the lanthanide series. Elements marked in red form clusters, elements marked in blue form stable divalent compounds with $4f^n5d^0$ electronic configurations

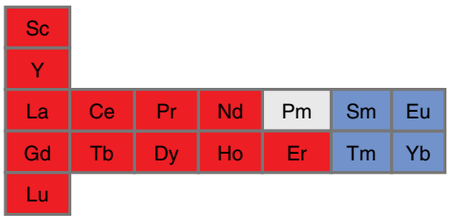

Figure 6 A periodic table of the rare earth elements with cluster-forming elements marked in red

The pattern as seen in Figure 5 may be transferred to a periodic table of the rare earth elements, see Figure 6. Only elements underlaid in red form clusters. The lower I_3 is, the easier it is to produce cluster complexes. Elements underlaid in blue form stable divalent compounds, for example $EuCl_2$; the divalent state with the electronic configuration $4f^n5d^0$ (with $n = 7, 14, 6, 13$ for R = Eu, Yb, Sm, Tm) has the highest stability and, thus, is the easiest to achieve when the third ionization potential is the highest. The divalent chemistry of these elements is alkaline-earth and saltlike; this is described in ***The Divalent State in Solid Rare Earth Metal Halides***.

3 SYNTHESIS

The synthesis of compounds of the lanthanides containing cluster complexes follows in general the same routes as described in ***The Divalent State in Solid Rare Earth Metal Halides***, the conproportionation route and the metallothermic reduction route, for example

$$4\ ScCl_3 + 8\ Sc + 3\ Os \rightarrow 3\ \{OsSc_4\}Cl_4,\ \text{or}$$
$$6\ Rb + 5\ PrCl_3 + 2\ C \rightarrow Rb[\{(C_2)Pr_5\}Cl_{10}] + 5\ RbCl \quad (1)$$

The reactions are carried out at high temperatures (up to 1000 °C) in sealed refractory metal containers (niobium, tantalum) over a prolonged period of time. Details may be found in the literature.[12–14] An advantage of the metallothermic reduction route is the simultaneous production of alkali-metal halides that may serve as a flux for crystal growth; and the disadvantage is that pure single-phase products are obtained only in rare cases. One severe drawback of both methods is that the phase diagrams are not known; therefore research in this area is largely based on intuition and serendipity.

4 LANTHANIDE HALIDES WITH EMPTY CLUSTERS

Sc_7Cl_{10}, LaI, and a number of sesquichlorides and bromides, R_2X_3, seem to be the only true binary reduced rare earth metal halides.[15,16] All the others that had once been claimed as monohalides, such as GdCl,[17] contain some endohedral atom (or atom group) in the center of a cluster, usually a metal octahedron.

Sesquihalides R_2X_3 (X = Cl, Br) have been observed for a number of R metals, namely, Sc, Y, Gd, Tb, and also La, Tm, Lu (which are doubtful), see Table 1. Although the crystal structures of Sc_2X_3 (X = Cl, Br) were never determined because the the crystals grow in extremely thin needles, there is no doubt about their existence, judging from phase diagram determinations. Sc_2Br_3, for example, the only compound in the $ScBr_3$/Sc system, melts incongruently at 880° C. The phase diagram of the $ScCl_3$/Sc system is similar.[18]

Gd_2Cl_3 was the first sesquichloride to be discovered and it is probably the best characterized.[19–22] It melts incongruently at 632 °C. Crystals grow in needles. This is reflected by the crystal structure. It is built from chains of edge-connected $\{Gd_6\}$ clusters surrounded by chloride ions (Figure 7). The parent cluster complex is of the $\{Gd_6\}Cl^i_8$ type. Owing to the trans-edge connection of the clusters, the number of chloride ions is reduced through redundancies from eight to six, according to the formulation $\{Gd_{4/2}Gd_{2/1}\}Cl_6$. The Gd-Gd distances are shortest for the connecting edge (335 pm), the others are considerably larger than 370 pm, suggesting weaker metal–metal bonding. Gd_2Cl_3 is a semiconductor and of only marginal stability with respect to the conproportionation reaction, $GdCl_3 + Gd = Gd_2Cl_3$, with $\Delta H° = -30 \pm 15$ kJ mol^{-1}.[22]

Except for Sc_2Cl_3 (= $ScCl_{1.5}$) a slightly further reduced scandium chloride, $ScCl_{1.43}$ (= Sc_7Cl_{10}) was secured that may, as with Gd_2Cl_3, be derived from the parent $\{R_6\}X_8$ cluster complex. Parallel chains of edge-connected $\{Sc_6\}$ octahedra are further connected to double chains as shown in Figure 8; an additional scandium atom resides in octahedral chloride interstices, in accord with the formulation $\{Sc_6\}Cl_{10}Sc$.[23] Again, the edge-shared Sc–Sc distances are the shortest, only 315 pm due to the smaller scandium atoms.

Other reduced scandium halides such as ''Sc_7Cl_{12}'' and ''ScCl'' are not free of interstitial atoms (H, C, N) although ''ScCl'', which crystallizes just like ZrCl, has a double layer structure which would be the end member of further condensation of edge-connected octahedral chains.

Table 1 Binary reduced rare earth metal halides

	Chloride	Bromide	Iodide
Scandium	Sc_2Cl_3, **Sc_7Cl_{10}**	Sc_2Br_3	—
Yttrium	**Y_2Cl_3**	Y_2Br_3	—
Lanthanum	La_2Cl_3	—	**LaI**
Gadolinium	**Gd_2Cl_3**	**Gd_2Br_3**	—
Terbium	**Tb_2Cl_3**	**Tb_2Br_3**	—
Thulium	Tm_2Cl_3	—	—
Lutetium	Lu_2Cl_3	—	—

Bold letters: Structure determined from single crystal data.

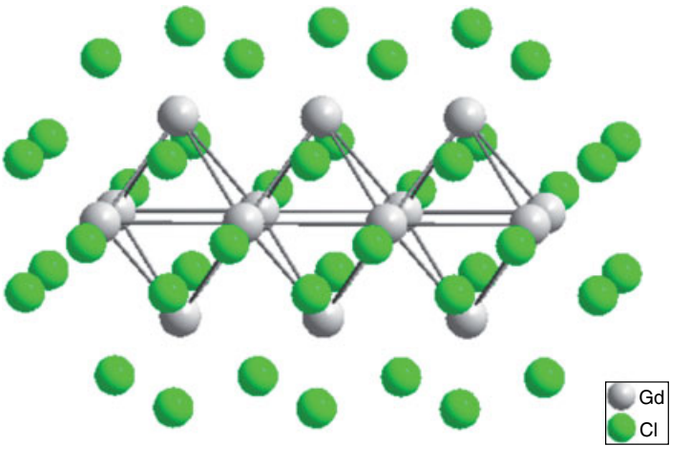

Figure 7 Chains of edge-connected $\{Gd_6\}$ octahedra surrounded by chlorido ligands in the crystal structure of Gd_2Cl_3

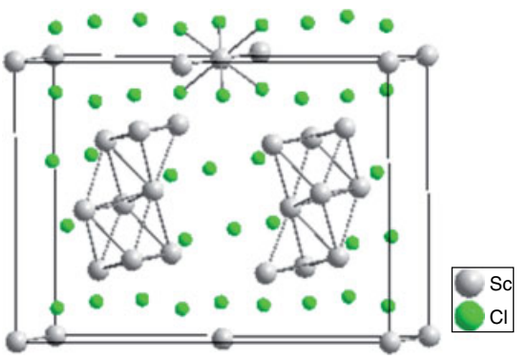

Figure 8 Double chains in the crystal structure of Sc_7Cl_{10} (a) and their connection through an additional scandium atom with the chains running down [010] (b)

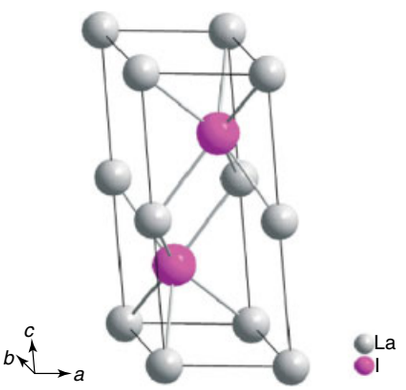

Figure 9 Crystal structure of NiAs-type lanthanum monoiodide, LaI

Lanthanum shows a unique feature with the only true monohalide of the rare earth elements, LaI.[24] It was first obtained by a conproportionation reaction and quite recently stabilized with aluminum as $(La_{1-x}Al_x)I$ with $x < 0.15$. Through metallothermic reduction of LaI_3 and LaI_2, it is now available as pure phase.[25] LaI crystallizes with the NiAs type of structure (Figure 9), although with an unusual c/a ratio of 2.47. There are two electrons available for La–La bonding. The bonding interactions are stronger parallel (001), reflected by d(La–La) = 393 pm, than in the [001] direction, d(La–La) = 485 pm. LaI shows metallic behavior.

5 HALIDES WITH CLUSTER COMPLEXES CENTERED BY ENDOHEDRAL ATOMS

The vast majority of metal-rich rare earth-metal halides form clusters $\{R_x\}$ that incorporate an atom Z, or a small atom group, in the center of the cluster, hence heteroatomic clusters $\{ZR_x\}$ need to be considered. These clusters are surrounded by ligands, usually halido ligands X^- of the triad chloride, bromide, and iodide. Figure 10 depicts such an isolated cluster complex $[\{ZR_6\}X^i_{12}X^a_6]^{n-}$.

In these cluster complexes, the endohedral atom Z is considered as the central atom (be it a nonmetal or a metal atom), which is surrounded by metal atoms R with a coordination number of—in the majority of cases—six (CN_6), as shown in Figure 10. This $\{ZR_6\}$ unit is a complex *anti* to Werner's classical complexes in that the charges, or better, polarities, of the central and the coordinating atoms are opposite to those in Werner complexes. We shall call it a cluster although it would not qualify as such according to a definition by Cotton, in that ''a metal atom cluster may be defined as a group of two or more metal atoms in which there are substantial and direct bonds between the metal atoms.''[1] In the present $\{ZR_6\}$ clusters, bonding interactions are mainly heteroatomic Z–R, with minor R–R contributions. This is symbolized by the thickness of the ''bonding sticks''

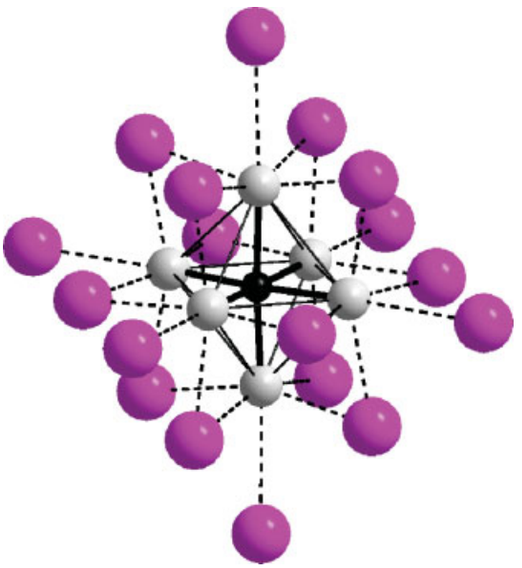

Figure 10 Isolated cluster complex with endohedral atom, $[\{ZR_6\}X^i{}_{12}X^a{}_6]^{n-}$

in Figure 10. Further polar bonding results from R···X interactions. In the following, $[\{ZR_6\}X^i{}_{12}X^a{}_6]^{n-}$ type cluster complexes are regarded as *anti*-Werner complexes,[4] for the following reasons.

In a typical Werner complex, such as in solid $[PtCl_6]K_2$, to use the original formulation (today we usually write $K_2[PtCl_6]$),[26] the central atom as the zeroth coordination sphere is surrounded by six chlorido ligands as the first coordination sphere followed by eight potassium cations in the second coordination sphere, see Figure 11. In a purely ionic description this would read $[(Pt^{4+})(Cl^-)_6](K^+)_2$, or simplified $[+-]+$.

In $Cs_2Lu_7Cl_{18}C$, as has been written previously, a single carbon atom (central atom, zeroth coordination sphere) is surrounded by an octahedral cluster of six lutetium atoms, which is written as $\{CLu_6\}$ to distinguish a Werner complex from an *anti*-Werner complex. This ''cluster'' is surrounded (in the second coordination sphere to the central carbon atom) by 12 chlorido ligands capping the edges of the cluster and 6 terminal chlorido ligands (capping the corners), and in third coordination sphere by 12 cesium cations. A seventh lutetium cation fills octahedral holes that are provided by the chlorido ligands in the crystal structure, see Figure 11. Thus, $Cs_2Lu_7Cl_{18}C$ should better be written as $[\{CLu_6\}Cl_{12}{}^iCl_6{}^a]Cs_2Lu$, as this formulation carries structural information. Note that $[\{CLu_6\}Cl_{12}{}^iCl_6{}^a]Cs_2Lu$ is also a Werner complex as the whole cluster $\{CLu_6\}$ could be considered a ''super central atom'' with coordination number 18. The anion $[\{CLu_6\}Cl_{18}]^{5-}$ needs to be called a ''cluster complex.'' In a purely ionic description, this compound would have to be formulated as $[\{(C^{4-})\ (Lu^{3+})_6\}(Cl^-)_{18}](Cs^+)_2(Lu^{3+})$. There would be one excess electron; of course, this is an oversimplified picture but it shows that the charges in the succession of coordination spheres move in a direction, $[\{-+\}-]+$, opposite to Werner's classical complexes.

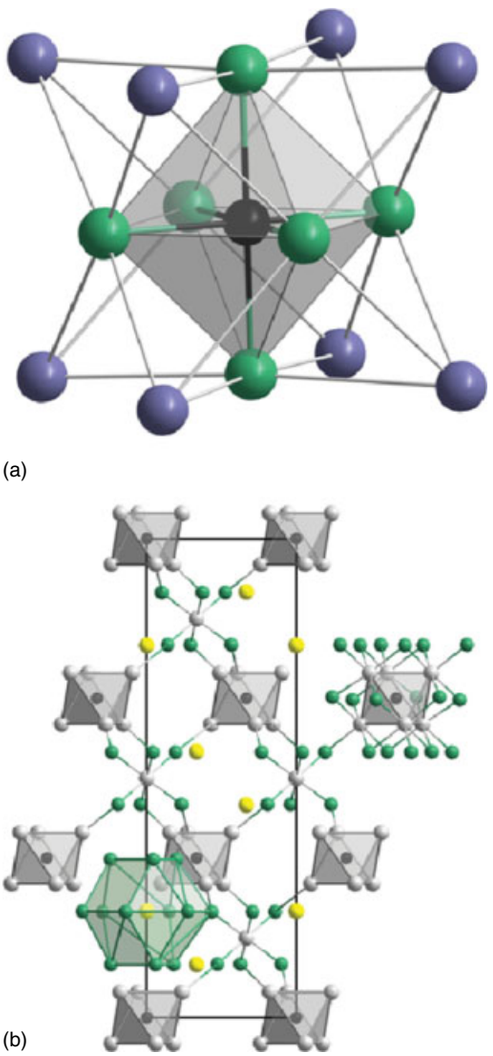

Figure 11 (a) Werner complex, $[PtCl_6]K_{8/4}$, with a central metal atom (Pt^{4+}) surrounded by six ligands (Cl^-) in the first and eight (K^+) in the second coordination sphere, hence with polarities $[+-]+$. (b) An analogous picture for the cluster complex salt $[\{CLu_6\}Cl_{12}{}^iCl_6{}^a]Cs_2Lu$ with polarities of $[\{-+\}-]+$, an *anti*-Werner cluster complex

Cluster complexes that obey Cotton's strict definition such as $[\{Nb_6\}Cl_{18}]K_4$ and $[\{Mo_6\}Cl_{14}]Cs_2$ have 16 and 24 electrons, respectively, for bonding interactions within the octahedral niobium and molybdenum clusters. In a VB picture, these electrons are consumed for eight two-electron-three-center (2e–3c) or 12 2e–2c bonds, situated in the eight triangular faces and the 12 edges of the respective octahedra.

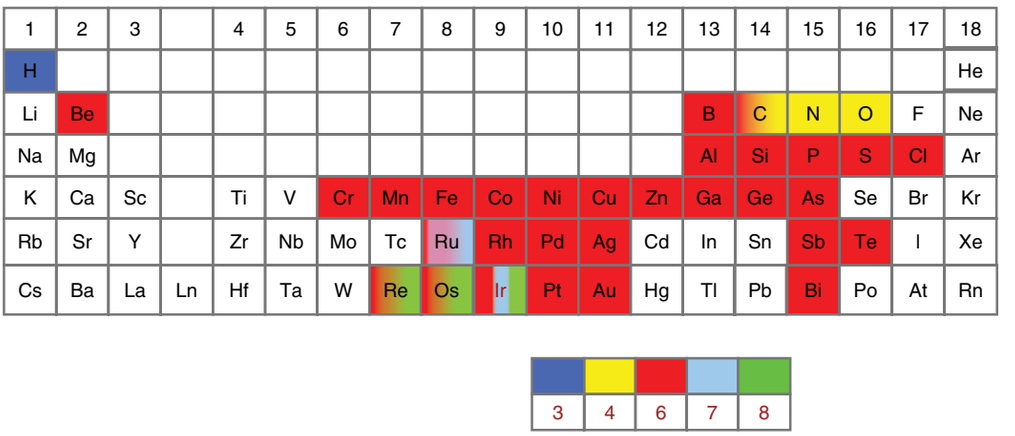

Figure 12 Endohedral atoms Z (colored for their different coordination numbers) as found in cluster complexes $[\{ZR_6\}X^i{}_{12}X^a{}_6]^{n-}$

Group 3 elements have only three VEs to contribute to intracluster bonding because the 4f electrons of the lanthanoid elements are rather corelike and can thus not be involved in bonding. Compounds such as $[\{\square Lu_6\}Cl_{18}]Cs_2$, $[\{\square Lu_6\}Cl_{18}]Cs_4$, or $[\{\square Lu_6\}Cl_{18}]Cs_2Lu$ would only have 2, 4, and 5 electrons for Lu–Lu bonding, which is much less than 16! The endohedral carbon atom is needed to contribute its four VEs. Still, with nine electrons, $[\{CLu_6\}Cl_{18}]Cs_2Lu$ is very electron poor and remains a mystery. As the carbon atom is more electronegative than the lutetium atoms, these nine electrons cannot be used for Lu–Lu bonding.

Therefore, bonding in the clusters that are discussed in this chapter is predominantly Z–R bonding. The paucity of electrons is also the reason that isolated cluster complexes are rare. The connection of clusters (mostly) via common edges to oligomers or extended structures (chains, layers) saves electrons and thereby contributes to the stability of these compounds.

An endohedral atom sequestered in a cluster needs space. Therefore, only hydrogen can be incorporated in triangles, but hydrogen atoms are also found in tetrahedra or octahedra (sometimes two H atoms in one octahedron, or seven capping statistically the eight faces). Oxygen, nitrogen, and carbon as electronegative atoms qualify for tetrahedral interstices; nitrogen and carbon are also found in octahedral clusters. Most of the other endohedral atoms see Figure 12 occupy octahedral interstices. Only a few clusters have higher nuclearities; large atoms such as ruthenium, osmium, and iridium are needed for coordination numbers of 7 and 8, only in extended structures.

5.1 Tetrahedral Clusters, $\{ZR_4\}$

Oxide-halides of the alkaline-earth-like divalent lanthanides, $\{OR_4\}X_6$ (R = Eu, Yb, Sm) are discussed in ***The Divalent State in Solid Rare Earth Metal Halides***. Although, these have the topology of cluster complexes with isolated $\{OR_4\}$ clusters, the R^{2+} ions have $4f^n5d^0$ configurations and the compounds are therefore best considered as ionic, $\{(O^{2-})(R^{2+})_4\}(X^-)_6$. There is, however, a lanthanum bromide, $\{ZLa_4\}Br_7$ (the nature of Z, be it O or N, is not really clear), with a structure similar to that of $\{OR_4\}X_6$, but the connection between the cluster complexes via common bromide ions is different in $\{ZLa_4\}Br_7$; Figure 13 shows one isolated $\{ZLa_4\}$ cluster and the surrounding ligands.[27]

Except for this monomeric cluster complex, there are tetrahedral clusters with Z = O, N that have edge-connected $\{ZR_4\}$ tetrahedra, either as dimers or chains. The dimers are not so frequent but have first been observed for $Gd_3NCl_6 = \{NGd_{2/2}Gd_{2/1}\}Cl_6$.[28] The dimers may be connected in different ways to chains. Most frequently observed is the connection via two trans-edges as in $Gd_2NCl_3 = \{NGd_{4/2}\}Cl_3$, see Figure 14. The composition $\{NR_2\}Cl_3$ is known for R = La, Cr, Pr, Nd, Gd, Y and comes with two structure types where the larger lanthanides form a more symmetric structure (R = La, Ce, Pr) than the smaller ones (R = Nd, Gd, Y).[29,30] The dimers may also be connected via four common vertices to a double chain as observed for another modification of Gd_2NCl_3 (named β). There are a number of other compositions that include trans-edge connected tetrahedral chains, for example, $[\{ZPr_{4/2}\}_2Cl_9]Na_2$[31–33] or $[\{ZLa_{4/2}\}_2I_8]Ba$ with Z = O, N.[27]

Although carbon atoms in tetrahedral clusters are rare, they have been found in the isolated cluster in $\{CCe_4\}Cl_8$[34] as well as in tetrahedral dimers (two tetrahedra sharing a common edge) in $\{C_2La_6\}Br_9$ and $\{C_2Pr_6\}Cl_{10}$.[35,36] They have also been found in the supertetrahedral molecular cluster complex $\{Sc_4C_{10}Sc_{20}\}I_{30}$; in this spectacular compound, an inner empty $\{Sc_4\}$ tetrahedron is surrounded by 10 carbon atoms such that a T2–$\{Sc_4C_{10}\}$ supertetrahedron appears, which is incorporated in a T3–Sc_{20} supertetrahedron; the $\{Sc_4C_{10}Sc_{20}\}$ cluster is enveloped in a truncated and hollow T4–I_{30} supertetrahedron, see Figure 15.[37] If viewed in an ionic model, $(Sc^{3+})_{24}(C^{4-})_{10}(I^-)_{30}$, there are two excess electrons that are believed, in a local bonding model, to reside

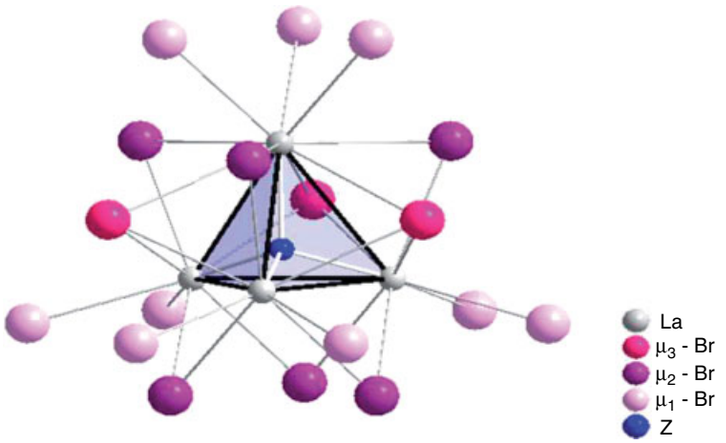

Figure 13 Isolated $\{ZLa_4\}$ clusters and their surrounding ligands in the crystal structure of $\{ZLa_4\}Br_7$

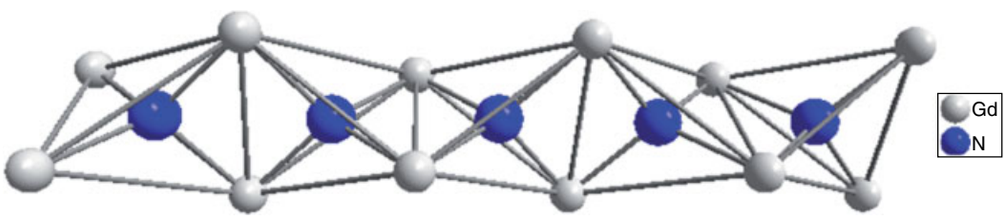

Figure 14 Edge-connected $\{ZR_4\}$ clusters in the crystal structure of, e.g., α-$\{NGd_{4/2}\}Cl_3$

in a 4c–2e orbital of the same shape as the inner $\{Sc_4\}$ cluster. This is then an analogous situation as in the naked $\{Au_{20}\}$ cluster, a T3 supertetrahedron with 20 electrons, consisting of 10 tetrahedra and thus with 10 4c–2e ''bonds.''[38,39]

5.2 Trigonal Bipyramidal Clusters, $\{ZR_5\}$

Two tetrahedra sharing a common face form a trigonal bipyramid, $\{R_5\}$. This appears to be an exceptional case, because it is only seen with a dicarbon unit centering the two tetrahedra and arranged along the threefold axis. This motif was first observed for $[\{C_2Pr_5\}Cl_{10}]Rb$, see Figure 16.[40] The cluster complex anion represents a three-dimensional network, $[\{C_2Pr_5\}Cl^{i-a}{}_{9/2}Cl^{a-i}{}_{9/2}Cl^{a-a-a}{}_{3/3}Cl^{a}{}_{3/3}]^-$, in which the Rb^+ cations are incorporated. There is a small class of compounds with the compositions $[\{C_2R_5\}X_{10}]A$ and $[\{C_2R_5\}X_9]$ with, in principle, A = K, Rb; R = La, Ce, Pr, Nd, X = Cl, Br, I.[40–45]

In all these compounds, the C–C distance is in the range of a single bond such that a C_2^{6-} ''anion'' can be assumed or, in other words, this ethanide unit contributes six electrons to intracluster bonding, which is mostly C–Pr interactions. All of these halides, $[\{C_2R_5\}X_{10}]A$ and $[\{C_2R_5\}X_9]$, have the same number of electrons, 12, for intracluster bonding. In an oversimplified picture, these 12 electrons could be attributed to six 3c–2e ''bonds,'' associated with the six triangular faces of the trigonal bipyramid.

5.3 Monomeric Octahedral Clusters, $\{ZR_6\}$

By far, the largest group of reduced rare earth metal halide cluster complexes contains octahedral $\{ZR_6\}$ clusters. They may be distorted directing to a trigonal prism or two tetrahedra sharing a common edge. We will, however, not trouble ourselves with these peculiarities, as important as they might be for the ''fine structure'' of chemical bonding in these metal-rich compounds.

Isolated octahedral clusters are scarce. There appears to be only one example, $Cs_2Lu[\{CLu_6\}Cl_{18}]$, in which not only the $\{CLu_6\}$ cluster is isolated but also the $[\{CLu_6\}Cl_{18}]^{5-}$ cluster complex unconnected.[46] The most prolific families with isolated clusters are the so-called 7–12 and 6–10 type compounds, halides of the compositions $\{ZR_6\}X_{12}R$ and $\{ZR_6\}X_{10}$. These are mostly iodides; for the 6–10 type, bromides are equally frequent, perhaps a packing problem.[47]

The crystal structure of the $\{ZR_6\}X_{12}R$ type consists of $\{ZR_6\}$ ''octahedra'' of 3 or usually –3 symmetry. These are surrounded by 18 X^- ligands that connect the cluster complexes to a three-dimensional structure according to $\{ZR_6\}X^{i}_{6/1}X^{i-a}{}_{6/2}X^{a-i}{}_{6/2}$ with additional R^{3+}

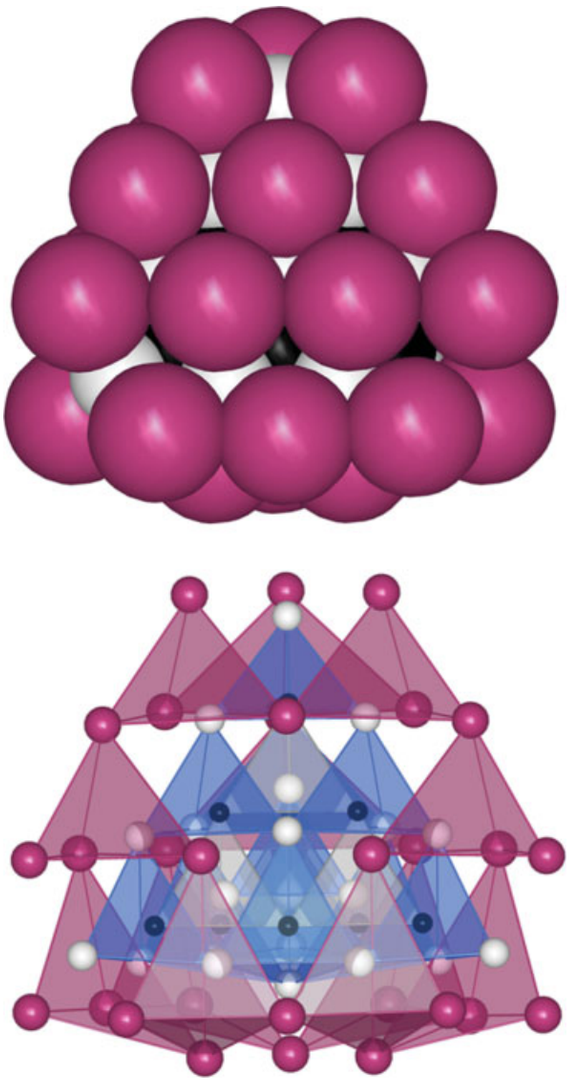

Figure 15 The $\{Sc_4C_{10}Sc_{20}\}I_{30}$ cluster complex molecule shown both as a space filling and a polyhedral model

in octahedral holes. Figure 17 shows, for the example of $\{IrEr_6\}I_{12}Er$, the sequence of one $\{IrEr_6\}I^i{}_{12}I^a{}_6$ cluster complex and two connected $[ErI_6]$ octahedra. The connection of the cluster complexes with each other is depicted in Figure 18. In $\{IrEr_6\}I_{10}$, for example, the connectivity between the cluster complexes is more pronounced, according to $\{IrEr_6\}I^i{}_{2/1}I^{i-i}{}_{4/2}I^{i-a}{}_{6/2}I^{a-i}{}_{6/2}$, see Figure 19. Endohedral atoms that have been observed for both types are mostly group 8–10 metal atoms, also B, C, and N for the 7–12 type.[47–50] C_2 is also an option as $\{C_2Dy_6\}I_{12}Dy$ shows.[51] Rare earth elements that form these two types of compounds are, in principle, all that are marked red in Figure 6. Electron counts, i.e., the number of electrons that are available for intracluster Z–R bonding, are between 11 and 14 for main-group Z and from 15 to 21 for transition-metal Z atoms.

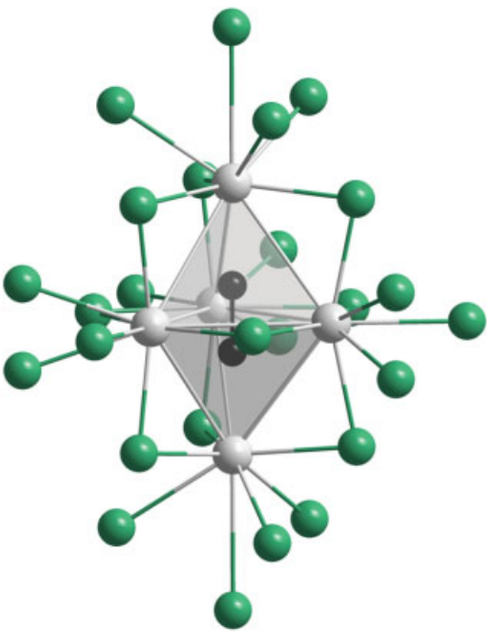

Figure 16 The cluster complex $\{C_2Pr_5\}Cl_{24}$ as it appears in the crystal structure of $[\{C_2Pr_5\}Cl_{10}]Rb$

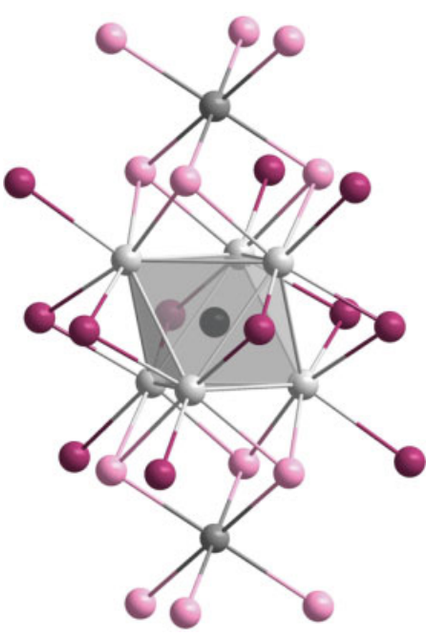

Figure 17 Cluster complex $\{IrEr_6\}I^i{}_{12}I^a{}_6$ connected with $[ErI_6]$ octahedra in $\{IrEr_6\}I_{12}Er$

Isolated clusters are also found in compounds such as $\{C_2Sc_6\}I_{11}$ or $\{RuY_6\}I_{10}$ with different connections of the 6–12 clusters to chains.[49,52] During the exploration of the

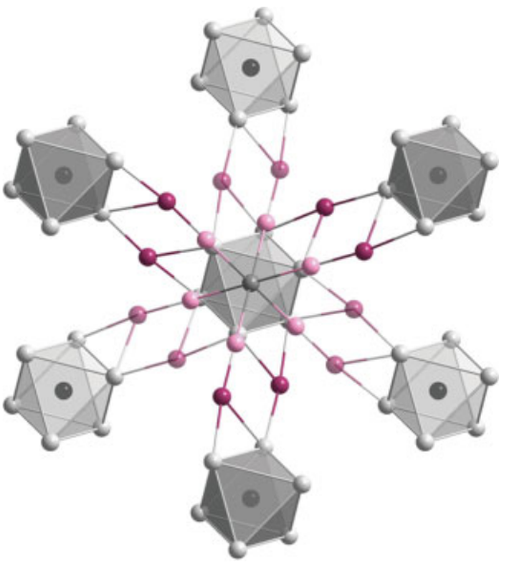

Figure 18 Interconnection of the cluster complexes $\{IrEr_6\}I^i{}_{12}I^a{}_6$ in $\{IrEr_6\}I_{12}Er$

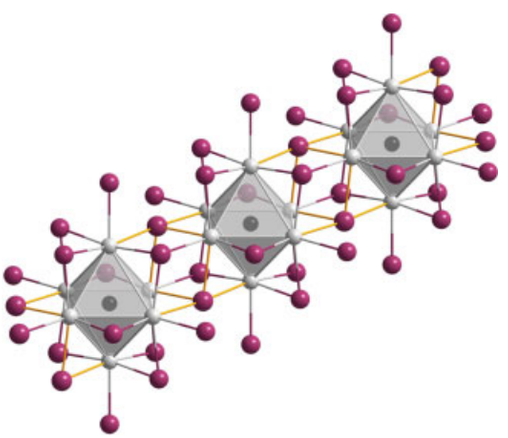

Figure 19 Interconnection of the cluster complexes $\{IrEr_6\}I^i{}_{12}I^a{}_6$ in $\{IrEr_6\}I_{10}$

metallothermic reduction of rare earth metal trihalides with alkali metals, a small number of compounds with isolated clusters have been obtained, all with single carbon or dicarbon units sequestered in an octahedron of metal atoms R = Sc, Pr, Er, Lu, for example, $[\{CEr_6\}I_{12}]Cs$ or $[\{C_2Pr_6\}I_{13}]Cs_4$. Electron counts are low, between 9 in $[\{CLu_6\}Cl_{18}]Cs_2Lu$ and 15 in $[\{C_2Pr_6\}I_{13}]Cs_4$.[53]

5.4 Oligomeric Clusters

Two octahedra sharing a common edge have first been found for $Gd_5Cl_9C_2 = \{(C_2)_2Gd_{10}\}Cl_{18}$.[54] In its structure

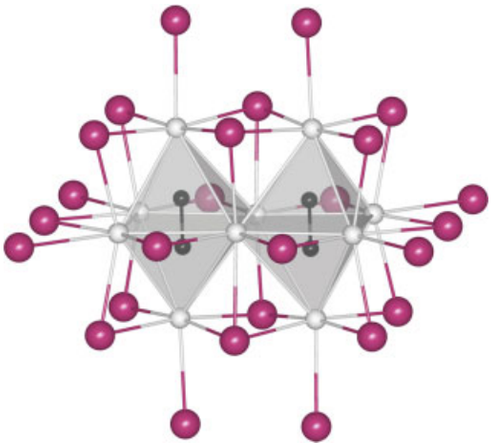

Figure 20 The $\{(C_2)_2R_{10}\}X_{26}$ dimer as it appears for example in $Cs[\{(C_2)_2Er_{10}\}I_{18}]$

and the structures of a number of ternary and quaternary halides with R = Gd, Tb, Er, Y, C_2 dumbbells as the endohedral unit are observed, see Figure 20 (boron and transition metal atoms were also observed as Z). In all of these, the parent unit $\{(C_2)_2R_{10}\}X_{26}$ is connected via halide bridges to three-dimensional structures, such that a halide stoichiometry between X_{16} and X_{21} is achieved.[53] An example for the highest halide content, and thus with the least connections of the dimers via halide bridges is $Cs_3[\{(C_2)_2Tb_{10}\}Cl_{21}] = Cs_3[\{(C_2)_2Tb_{10}\}Cl^i{}_{18/1}Cl^{i-i}{}_{2/2}Cl^{i-a}{}_{2/2}Cl^{a-a}{}_{2/2}]$.[55]

Two types of trimers were recently found. Open, trans–trans edge-connected trimers in $\{(C_2)_3R_{14}\}I_{20}$ with R = La, Ce, Pr,[56,57] see Figure 21. There is evidence from high-resolution transmission microscopic pictures that higher all-trans-edge connected oligomers exist before the infinite chains appear. Closed trimers have been observed for the first time for $\{Ir_3Gd_{11}\}Br_{15}$; the $\{Ir_3Gd_{11}\}$ part of the structure is isostructural with $\{O_3Cs_{11}\}$, see Figure 21.[58]

Two types of tetramers have been observed in crystal structures, but neither of them are all trans-edge connected. Rather the connection is trans–cis–trans in the tetrameric units $\{Z_4R_{16}\}X_{36}$ (Figure 22) that appear in $\{B_4Tb_{16}\}Br_{23}$[59] and $\{Ru_4Gd_{16}\}Br_{23}$[60]. In both compounds B and Ru atoms, respectively, center R_6 octahedra; the endohedral atoms build a rhombus. B–B distances within that rhombus are around 410 pm, whereas Ru–Ru are much shorter, with only 340 pm for the short diagonal and 370 pm for the edges. This hints at much stronger Ru–Ru than B–B bonding.

In an alternative, closed tetramer that was first observed for $\{Ru_4Y_{16}\}I_{20}$,[61] the endohedral atoms form a tetrahedron. The parent unit has the composition $\{Z_4R_{16}\}X_{36}$. There is a remarkable structural diversity with compositions as shown in Table 2.[61–67] Especially remarkable is the composition ZR_5X_7, for example $\{Ru_4Ho_{16}\}I_{20}\{\square Ho_4\}I_8$ (Figure 23), as it not only contains the iodide-bridged tetramer $\{Ru_4Ho_{16}\}I_{36}$ but also an empty tetrahedral cluster $\{\square Ho_4\}I_8$

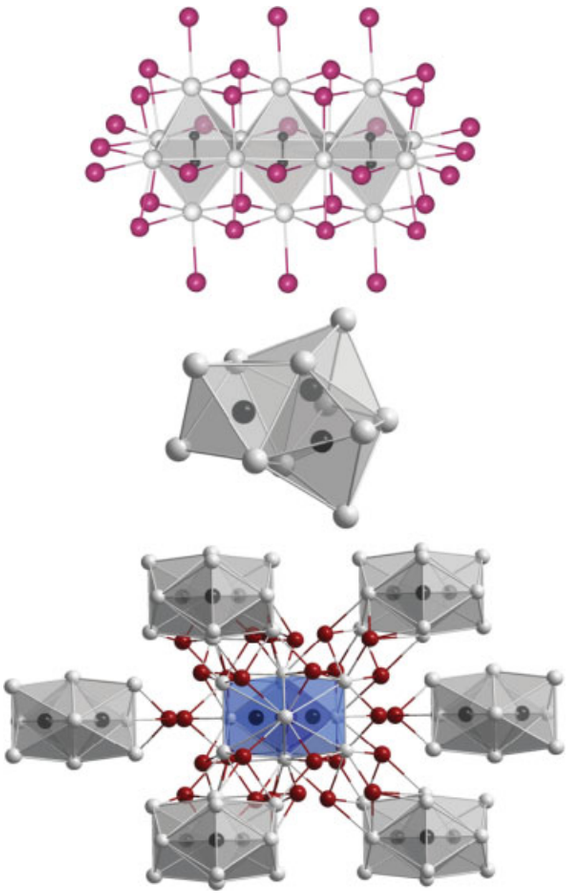

Figure 21 Open and closed trimers as they appear in, for example, $\{(C_2)_3Pr_{14}\}I_{20}$ and $\{Ir_3Gd_{11}\}Br_{15}$

which is isostructural with that first found in PrI_2-V.[68] When scaled to one endohedral atom Z, all these clusters have 15 ± 1 cluster-based electrons.

Hetero-endohedral cluster tetramers have been observed in $\{(C_2)_2(O)_2Dy_{14}\}I_{24}$. The terameric units $\{(C_2)_2(O)_2Dy_{14}\}I_{32}$ (Figure 24) are connected via i–a and a–i bridges to chains.[69]

Finally, spectacular pentameric units have been observed for $\{Ru_5La_{14}\}Cl_{20}$[70] and $\{Ru_5La_{14}\}_2Br_{39}$ (Figure 25).[71]

5.5 Single and Double Chains of Clusters

An infinite extension of the dimers, trans-trimers, and the trans–cis tetramers leads to chains, either linear or zigzag. In all cases, (less or more distorted) octahedral clusters $\{ZR_6\}$ are connected via common edges to chains in accord with the general formula $\{Z_xR_{4x+2}\}$; with $x \to \infty$, the formula type $\{ZR_4\}X_6$ results. There is a slowly growing number of examples, and they can be divided in three groups: I represents

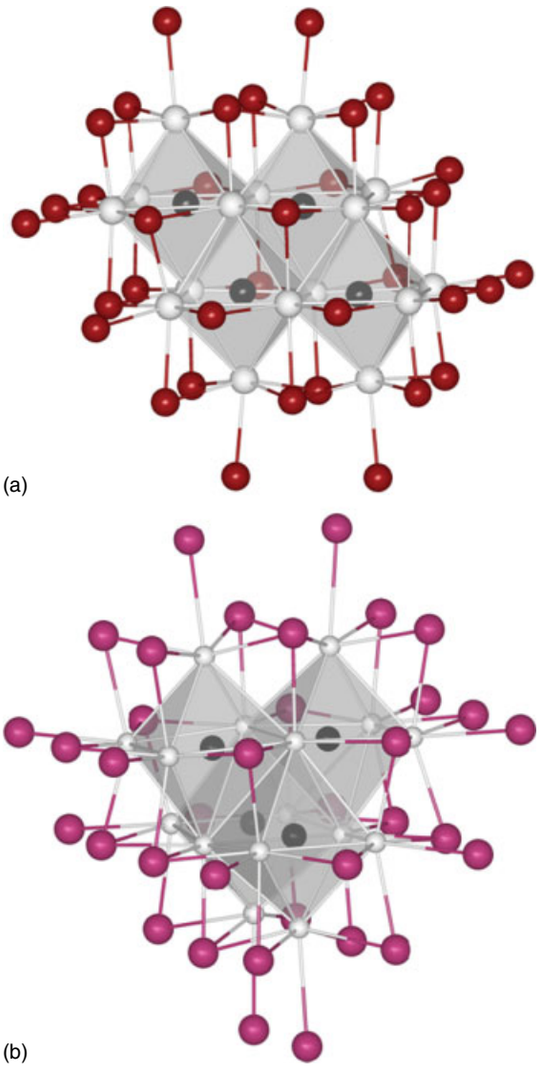

Figure 22 Two tetramers, $\{Z_4R_{16}\}X_{36}$ (a) and $\{Z_4R_{16}\}X_{36}$ (b), as they appear in, for example, $\{Ru_4Gd_{16}\}Br_{23}$ and $\{Ru_4Y_{16}\}I_{20}$, in which the endohedral Ru_4 tetramers build a rhombus and a tetrahedron, respectively

Table 2 Cluster complex tetramers $\{Z_4R_{16}\}X_{36}$ as incorporated in four different compositions

	Examples	$n(e^-)$
ZR_4X_5	$\{Fe_4Sc_{16}\}X_{20}$ (X = Cl, Br)	15
	$\{Ru_4Y_{16}\}X_{20}$ (X = Br, I)	15
	$\{Os_4Sc_{16}\}Br_{20}$	15
ZR_4X_6	$\{Ir_4Y_{16}\}Br_{24}$ (X = Cl, Br)	15
ZR_5X_7	$\{Z_4Sc_{16}\}Br_{20}\{\square Sc_4\}Br_8$ (Z = Mn, Fe, Ru, Os)	15/16
	$\{Mn_4Gd_{16}\}I_{20}\{\square Gd_4\}I_8$	15
	$\{Ru_4Ho_{16}\}I_{20}\{\square Ho_4\}I_8$	16
ZR_5X_9	$\{Z_4Sc_{16}\}Cl_{24}(ScCl_3)_4$ (Z = Ru, Os, Ir)	14/15
	$\{Z_4Y_{16}\}Br_{24}(YBr_3)_4$ (Z = Ru, Ir)	14/15
	$\{Z_4Tb_{16}\}Br_{24}(TbBr_3)_4$ (Z = Rh, Ir)	15

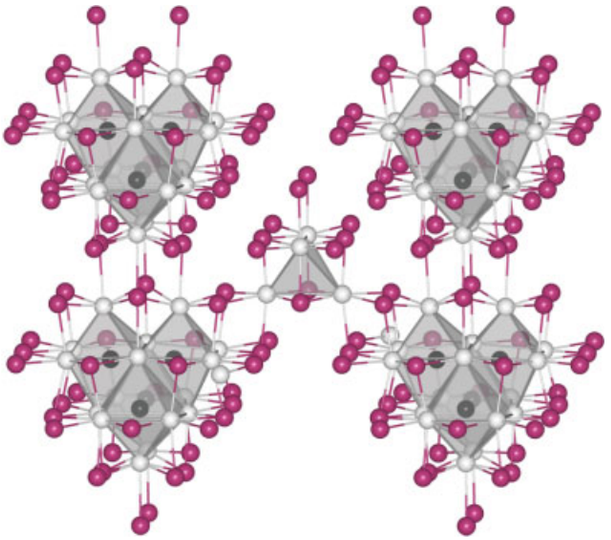

Figure 23 Part of the crystal structure of $RuHo_5I_7 = \{Ru_4Ho_{16}\}I_{20}\{\square Ho_4\}I_8$, exhibiting the empty $\{Ho_4\}$ cluster in the center

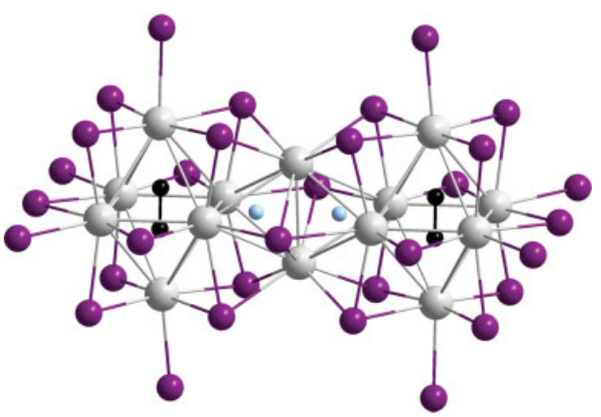

Figure 24 The tetrameric hetero-endohedral unit $\{(C_2)_2(O)_2Dy_{14}\}I_{32}$, as observed in $\{(C_2)_2(O)_2Dy_{14}\}I_{24}$ and $\{(C_2)_2(O)_2Dy_{12}\}I_{18}$

a rather highly symmetric chain, Figure 26, and was observed for $\{ZSc_4\}Cl_6$ (Z = B, N) and $\{SiR_4\}Br_6$ (Z = Gd, Tb).[50,72,73] The inclusion of C_2 dumbbells oriented along one of the fourfold axes of the R_6 octahedra leads to elongations in this direction, for which two varieties have been observed, IIa, $\{(C_2)R_4\}I_6$ (Dy, Er)[66,74] and IIb, $\{(C_2)Sc_4\}I_6$,[52] (Figure 26). Small clusters, $\{Sc_6\}$, and large ligands, I^-, cause the most severe distortions of the previously linear chain. In group III, edge-connected dimers are connected via further edges to a zigzag chain (Figure 26).[67,75–77]

In the chains of group IIa, octahedra are, alternatively, elongated and compressed. The compressed octahedra can also be viewed as two tetrahedra sharing a common edge, with the edge passing through the middle of the C–C bond.

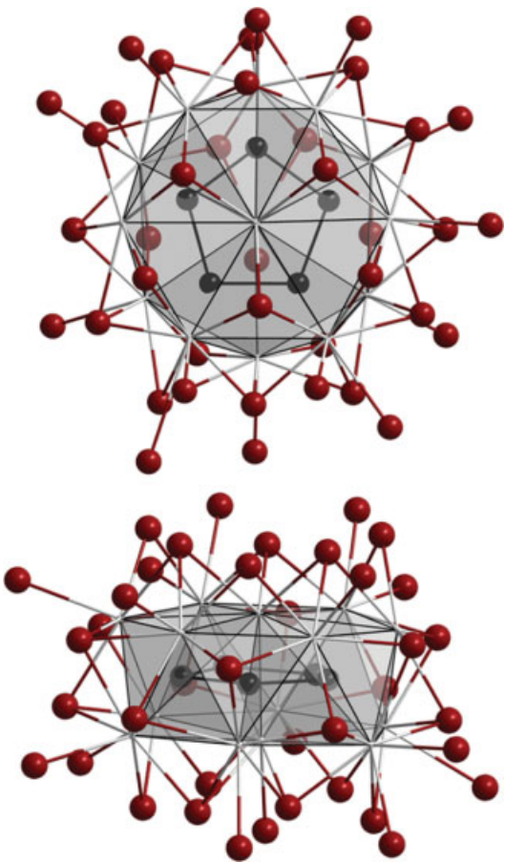

Figure 25 The pentameric cluster complex unit $\{Ru_5La_{14}\}Br_{39}$ (top and side views) in the crystal structure of $\{Ru_5La_{14}\}_2Br_{39}$

One octahedron added and two carbon atoms substituted by oxygen atoms, lead to a tetrameric unit, for example $\{(C_2)_2(O)_2Dy_{14}\}I_{32}$, see Figure 24. These tetramers may be connected via common edges to an infinite chain, as observed in $\{(C_2)_2(O)_2Dy_{12}\}I_{18}$ (Figure 27) such that (elongated) octahedra (O) and tetrahedra (T) are all edge-connected with a sequence of $\cdots$OOTT$\cdots$.[69]

Chains as observed for group I, $\{ZSc_4\}Cl_6$ (Z = B, N) and $\{SiR_4\}Br_6$ (Z = Gd, Tb), are also observed in compounds with other stoichiometries, $\{ZR_4\}X_5$ and $\{ZR_4\}X_8R$, respectively. In the beginning, both formula types were addressed as binaries, for example Er_4I_5 and Sc_5Cl_8.[78–85] In $\{ZR_4\}X_5$ type compounds, for example, $\{CY_4\}I_5$ or $\{SiGd_4\}I_5$, the chains are further connected via halide ligands to layers, see Figure 28. In $\{ZR_4\}X_8R$, the chains are connected via additional metal halide octahedra, as for example in $\{CSc_4\}Cl_8Sc$, see Figure 28.

Single chains similar to those as observed in group III $\{ZR_4\}X_6$ halides are also found for the $\{(C_2)R_4\}X_{5.67} = \{(C_2)R_4\}_3I_{17} = R_{12}(C_2)_3I_{17}$ family, R = La, Cr, Pr, Nd, Gd, Dy, with trans–cis–cis connections throughout the corrugated chains, see Figure 29.[86–88]

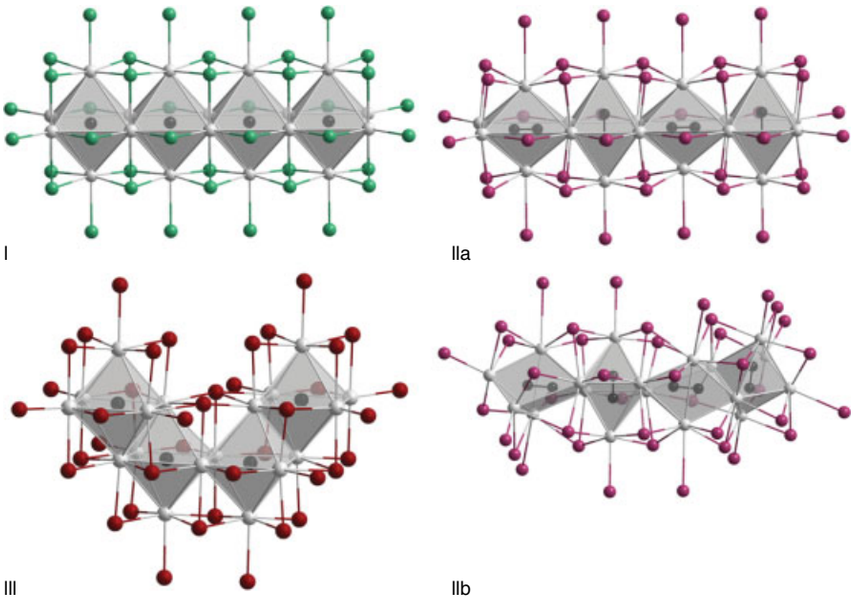

Figure 26 The variety of chains of edge-connected $\{ZR_6\}$ octahedra in $\{ZR_4\}X_6$ type compounds

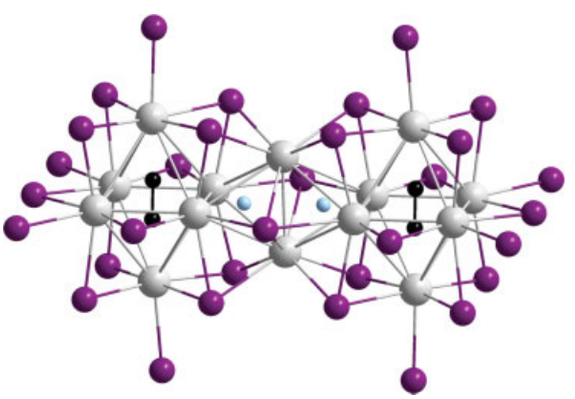

Figure 27 Part of the infinite chain of edge-connected octahedra and tetrahedra ($\cdots$OTTO$\cdots$) as observed in $\{(C_2)_2(O)_2Dy_{12}\}I_{18}$

The $\{ZR_3\}X_3$ stoichiometry is found for the usual suspects, R = La, Ce, Pr, Gd, Tb, Y, Er, and with a great variety of endohedral atoms, Z = B, C, C_2, Si, P, Ga, As, Sb, Pb, Co, Ru, Rh, Os, Ir, Pt, Au; iodides and bromides are more frequent than chlorides, so far. $\{CGd_3\}Cl_3$ was perhaps the first to be observed.[89] Its structure is also known from the insulator $\{PCa_3\}I_3$ and may be understood as an ordered and defective derivative of the rocksalt type of structure. The structure is still cubic, although noncentrosymmetric in space group $I4_132$ and can be understood as built of interpenetrating edge-connected helical chains, see Figure 30. An orthorhombic variant ($C222_1$) has been observed with C_2 units for $\{(C_2)R_3\}Br_3$ (R = La, Ce).[90]

The chains as they were observed first for monoclinic $\{RuPr_3\}I_3$[91,92] can either be understood as if $\{ZR_4\}X_6$ type single chains were connected to a double chain, or, likewise as zigzag chains of edge-connected octahedra, see Figure 31. The Z–R distances are rather uniform in $\{RuPr_3\}I_3$ but the relative sizes of the Z and R atoms seem to have some effect on their spread. Distortions of the edge-connected $\{ZR_6\}$ octahedra direct at monocapped trigonal prisms, see Figure 31. Peculiar R/Z/X size ratios appear to be responsible for the degree of distortion and the actual space group symmetry. Distortions appear to be larger for bromides and especially chlorides. $\{RuPr_3\}Cl_3$ is an example for a pronounced distortion that, however, leads to a higher space group symmetry (Pnma).[93] When moving from $\{RuPr_3\}I_3$ (almost undistorted edge-connected octahedra) on to $\{RuPr_3\}Cl_3$ (face-sharing distorted monocapped trigonal prisms), these distortions also have their effect on the electronic structure; for example, Ru–Ru bonding is negligible in $\{RuPr_3\}I_3$, whereas it is rather pronounced in $\{RuPr_3\}Cl_3$, although there are also considerable antibonding interactions closer to the Fermi level, see Figure 32.[94]

As just mentioned for $\{ZR_3\}X_3$ type compounds, the edge-connected zigzag chains $\{ZR_{6/2}\}$ may also be understood as double chains of edge-connected single chains, $\{ZR_4\} = \{ZR_{2/1}R_{4/2}\} \rightarrow \{ZR_{1/1}R_{2/2}R_{3/3}\}$. Such double chains were first observed for the binary Sc_7Cl_{10}, see Chapter 4. With good approximation, the same structure is adopted by $\{ZSc_3\}_2Cl_{10}Sc$ with Z = C, N, see Figure 33.[95,96] There is a 7% volume decrease from $\{Sc_3\}_2Cl_{10}Sc$ to $\{CSc_3\}_2Cl_{10}Sc$ attesting for the contraction of the scandium clusters due to C/N–Sc bonding.

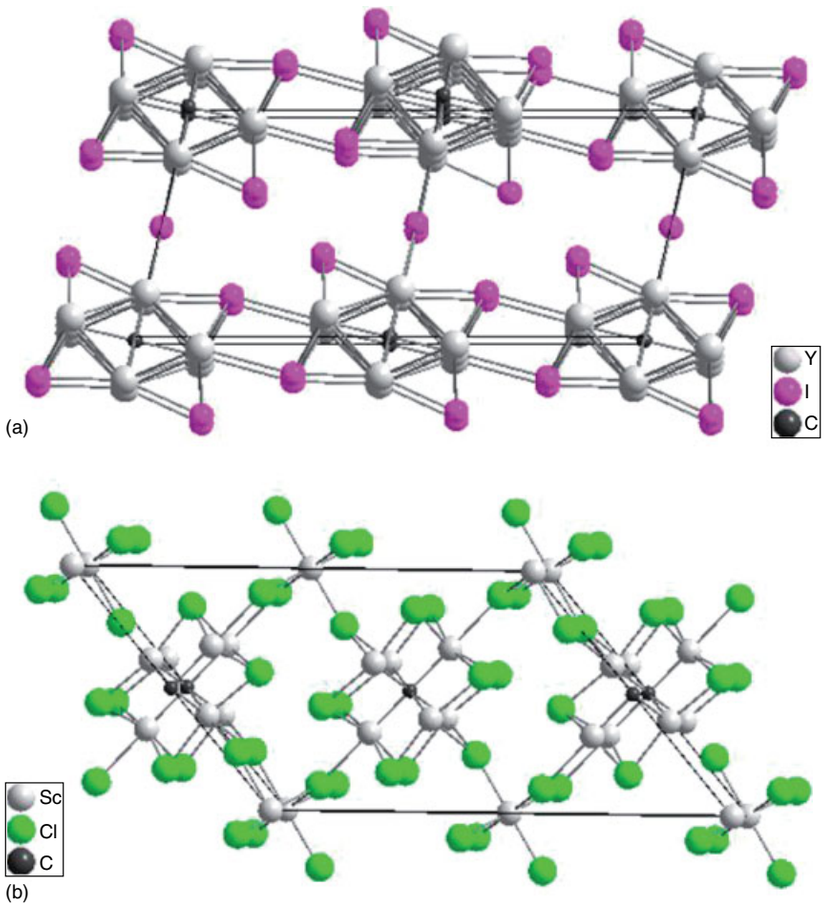

Figure 28 Chains as in type I $\{ZR_4\}X_6$ compounds connected further via halide, $\{ZR_4\}X_5$ type (a), and via additional metal halide octahedra as in the $\{ZR_4\}X_8R$ type (b)

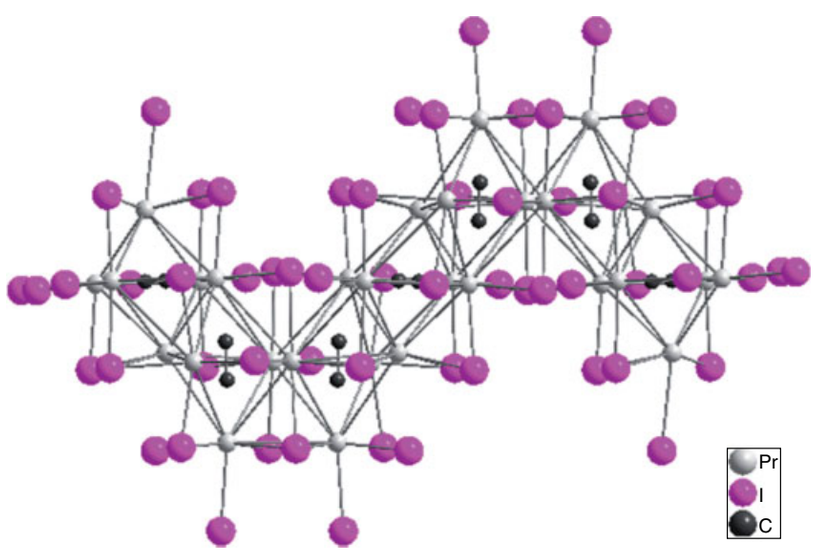

Figure 29 Corrugated chains of trans and cis edge-connected $\{(C_2)R_6\}$ clusters as observed in the crystal structures of the $\{(C_2)R_4\}_3I_{17} = R_{12}(C_2)_3I_{17}$ family, with R = La, Cr, Pr, Nd, Gd, Dy

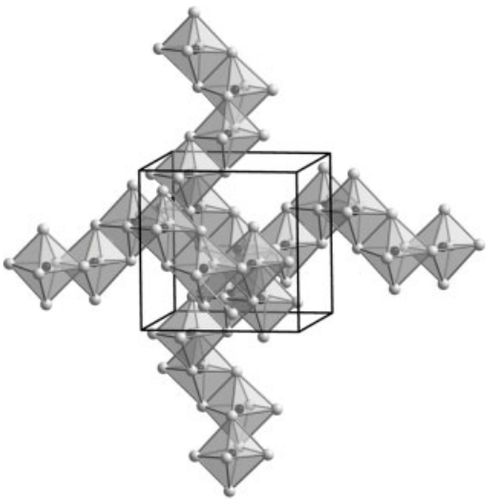

Figure 30 Helical, interpenetrating chains of edge-connected octahedra $\{ZR_{6/2}\}$ as observed, for example, in cubic body-centered $\{CGd_3\}Cl_3$

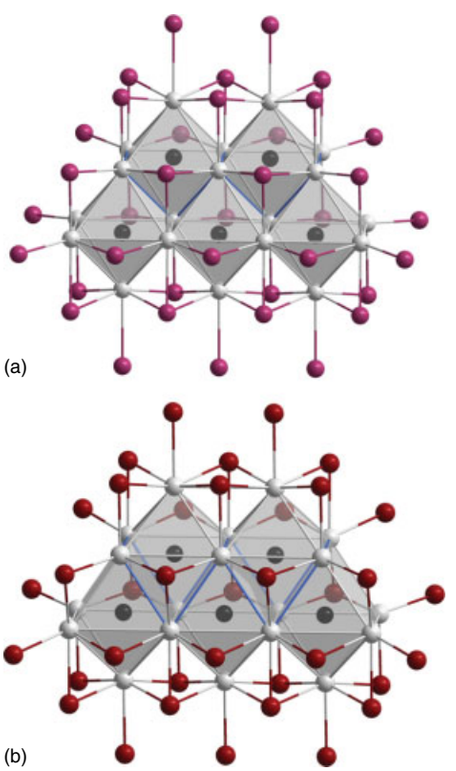

Figure 31 Zigzag chains of $\{ZR_6\}$ octahedra as they occur for example in $\{RuPr_3\}I_3$ (a) and their distortion to chains of face-sharing monocapped trigonal prisms as observed in $\{RuTb_3\}Br_3$ (b)

$\{ZR_{1/1}R_{2/2}R_{3/3}\}$ double chains are also known from bromides and iodides, which were formerly thought

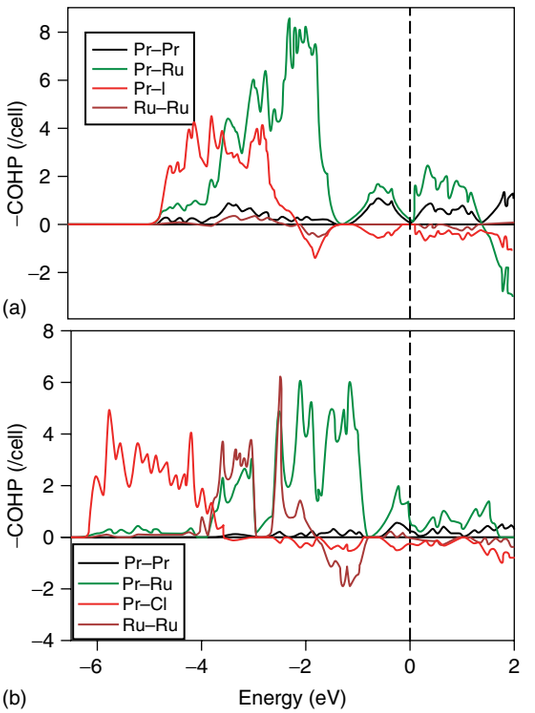

Figure 32 Crystal overlap Hamiltonian population (COHP) calculations for $\{RuPr_3\}I_3$ (a) and $\{RuPr_3\}Cl_3$ (b) showing the differences in bonding interactions

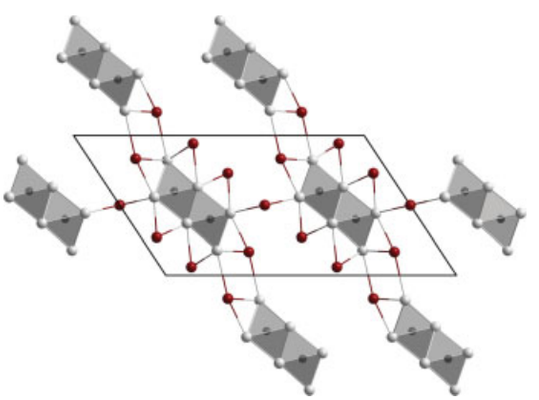

Figure 33 A view down the double chains $\{NSc_{1/1}Sc_{2/2}Sc_{3/3}\}$ (black) and their connection via $[ScCl_6]$ octahedra in the crystal structure of $\{NSc_3\}_2Cl_{10}Sc$

to be binaries, for example, Er_6I_7. The number of examples has increased in the meantime, and they appear to be all ternary compounds, $\{ZR_3\}_2I_7$, with Z always a C_2 dumbbell: $\{CR_3\}_2Br_7$ (R = Gd, Tb) and $\{CR_3\}_2I_7$ (R = Y, Gd, Er).[79,97–99] The double chains are surrounded by halido ligands and connected according to $\{CEr_{1/1}Er_{2/2}Er_{3/3}\}_2I^{i}{}_{4/1}I^{i-i}{}_{2/2}I^{a-i/i-a}{}_{4/2}$ to a three-dimensional structure, see Figure 34.

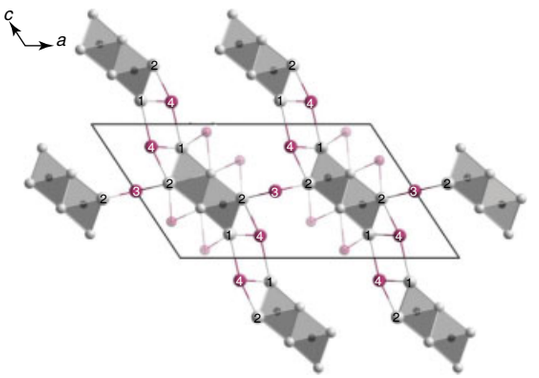

Figure 34 A view down the double chains $\{ZR_{1/1}R_{2/2}R_{3/3}\}$ and their connection via halide bridges in the crystal structures of $\{CR_3\}_2Br_7$ (R = Gd, Tb) and $\{CR_3\}_2I_7$ (R = Y, Gd, Er)

Further condensation to triple or quadruple chains has not been observed crystallographically, which is, by the way, the same with silicates. The next step of condensation is to build layers.

5.6 Layers

Layers were first found in ''GdCl'' that turned out to be a hydride of undetermined hydrogen content, $\{H_xGd_{6/6}\}Cl$.[17] Other than the hydride halides of the alkaline-earth-like rare earth metals, RHX (R = Eu, Yb, Sm; X = Cl, Br, I), which crystallize with the PbFCl type of structure, hydride halides $\{H_xR_{6/6}\}X$ with R = Sc, Y, La, Ce, Pr, Gd, Tb, Er, Lu[100] crystallize with one of two structure types, ZrCl or ZrBr.[101,102] They both contain four-layer slabs XRRX with hydrogen incorporated in the octahedral interstices between the RR metal double layers. The layers are two-dimensional, infinitely condensed chains of $\{ZR_6\}$ octahedra. Both structures need to be described in space group $R-3m$ with the four-layer slabs stacked in the ABC or the ACB fashion, hence reverse and observe in the [001] direction, see Figure 35. All compounds are ''nonstoichiometric,'' they have a homogeneity range, with $x = 1.0$ (for $\{H_xR\}X$) being the upper limit. They are all two-dimensional metals. Higher hydrogen contents lead to insulators with RH_2X being the upper limit, transparent ionic compounds, $(R^{3+})(H^-)_2(X^-)$. The $\{H_xR_{6/6}\}X$ type hydride halides may also be intercalated between the halide double layers with alkali metals, preferably Li and less Na.[103]

Equal four-layer slabs are also observed for carbide halides $\{CR_2\}X_2$ and $\{(C_2)R_2\}X_2$ with single carbon atoms and dicarbon units, respectively, residing in all of the octahedral interstices between the metal double layers. There are also three-layer slab structures of the composition $\{CR_2\}X$ in which one halide layer is missing such that the sequence is of the RRX type. In principle, they may be obtained with the same rare earth elements as the hydride halides.

The parent ZrBr type of structure appears to be preferred for $\{CR_2\}X_2$ type compounds (denoted 3R). The alternative is the so-called 1T structure type, whose identity period along [001] of the trigonal unit cell ($P-3m1$)

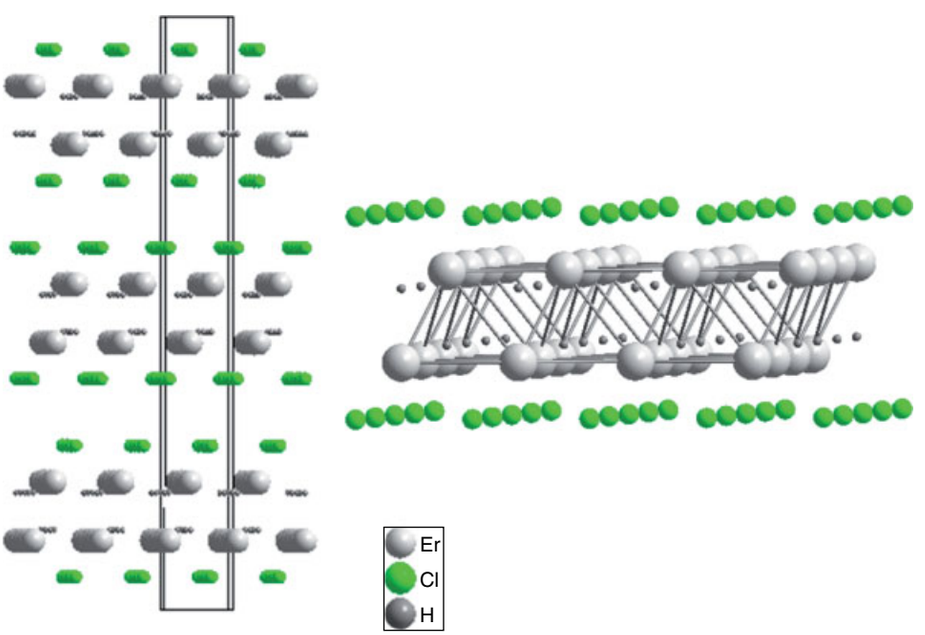

Figure 35 Schematic representation of the ZrCl and ZrBr types of structures in which the $\{H_xR_{6/6}\}X$-type rare earth hydride halides crystallize

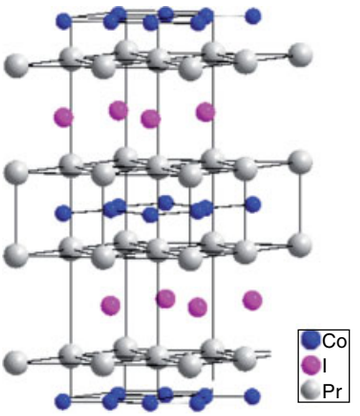

Figure 36 Crystal structure of $\{Co_2Pr_2\}I$ exhibiting the $\{CoPr_6\}$ clusters connected via common rectangular faces to layers sheathed by single iodide layers

corresponds to only one slab. For $\{CLu_2\}Cl_2$, both structures have been observed.[104,105] The only layered structure with nitrogen atoms in octahedral metal interstices seems to be $\{NSc_2\}Cl_2$. It crystallizes with the 1T structure type.[50]

Except for the nonmetal atoms H, C, and N, transition metal atoms have also been found as endohedral atoms in layered structures, for example Z = Fe, Co, Ni, Ru, Os. In principle, all rare earth elements with possible $5d^1$ configurations can adopt $\{Z_2R_2\}X$ compositions with X predominantly I, but Br is also possible. The . . . XRZ_2RX. . . layers are stacked such that trigonal prisms $\{R_6\}$ occur, which are all filled by Z atoms, see Figure 36 for the example of $\{Co_2Pr_2\}I$.[106] Ample investigations have been carried out for R = La, Pr, and Gd.[107–109] An alternative to this structure is that of $\{CGd_2\}Cl$, where $\{CGd_6\}$ octahedra share common edges. It may be understood as a stuffed *anti*-$CdCl_2$ derivative according to $\{CGd_2\}Cl = \{CdCl_2\}\square$.[110]

Layers do not have to be flat. They may be corrugated, waved, or steplike, as has been observed for a small number of mixed-interstitial iodides, $\{(C_3O)Y_7\}I_6$ and $\{(C_4O)R_9\}I_8$ (R = Y, Ho, Er, Lu), see Figure 37, and also for $\{C_3Gd_6\}Cl_5$.[111–113]

5.7 High-Coordinate Endohedral Atoms, $\{ZR_x\}$ with $x = 7, 8$

The vast majority of reduced rare earth metal halides incorporate nonmetal or metal atoms (or atom groups) in octahedral interstices, as we have seen, see also Figure 12. It requires large atoms to expand the coordination environment beyond a coordination number of six. For $\{RuPr_3\}Cl_3$, we have assigned CN = 7 to the ruthenium atom that resides off-center in a monocapped trigonal prism; this has been discussed in connection with $\{ZR_3\}X_3$ phases, see above. Atoms of the sixth-period elements are even larger, especially their 5d orbitals—which are needed to establish bonding interactions between Z and R—are more expanded. So far, rhenium, osmium, and iridium are the only metals found as endohedral atoms with CN = 8. The associated polyhedra can either be square antiprisms or cubes.

Compounds of the $\{ZR_4\}X_4$ type have been observed for $\{OsR_4\}Br_4$ with R = Y, Er as well as for $\{OsSc_4\}Cl_4$ and the higher symmetric $\{ReGd_4\}Br_4$.[114,115] In all compounds, square antiprisms of R atoms, encapsulating a Re/Os atom, share common faces to chains $\{ZR_{8/2}\}$, which are surrounded by and connected through halide anions, see Figure 38. These compounds have 15/16 cluster-based electrons, scaled per one Z.

A small number of variants of these face-sharing chain compounds have recently emerged, $\{Ir_3Sc_{12}\}Br_{16}$[114,115] in which square antiprisms and cubes in a 2 : 1 ratio share common square faces and $\{Os_5Lu_{20}\}I_{24}$[116] with a 4 : 1 ratio, see Figure 39. The number of electrons per Z is 16 for $\{OsSc_4\}Cl_4$,

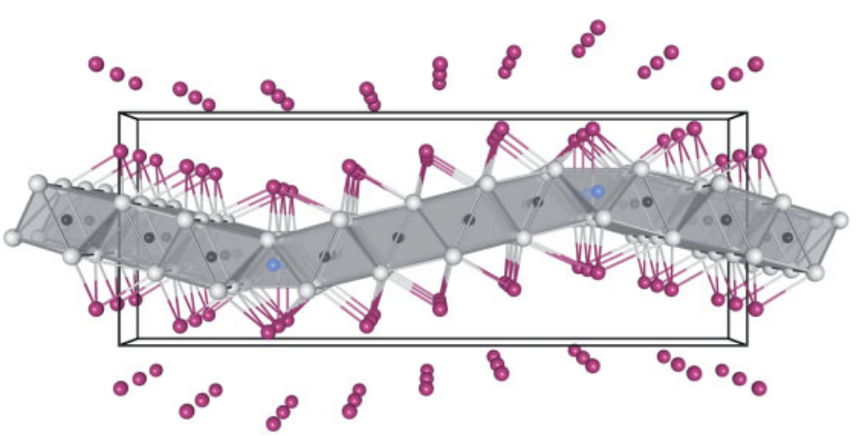

Figure 37 Corrugated layers as observed in $\{(C_4O)Y_9\}I_8$ with carbon atoms occupying octahedral interstices and oxygen atoms tetrahedral voids

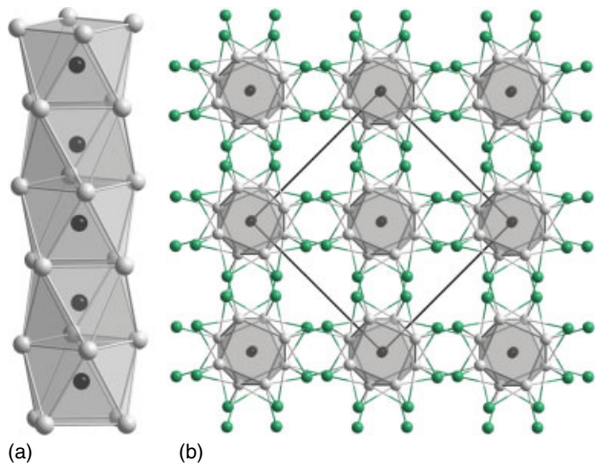

Figure 38 $\{OsSc_{8/2}\}$ chains of face-sharing square antiprisms (a) and their surrounding and connection in the crystal structure of $\{OsSc_4\}Cl_4$ and in the isostructural bromides $\{OsR_4\}Br_4$ (R = Y, Er) (b)

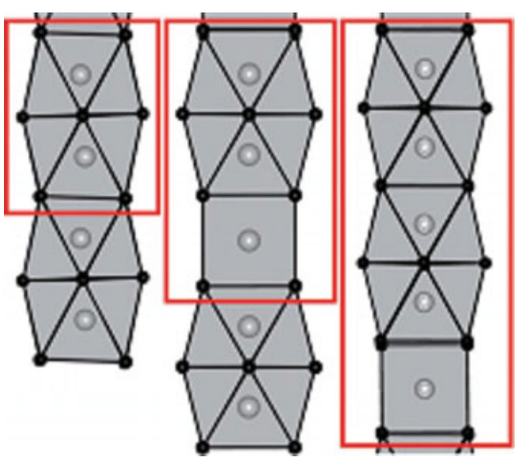

Figure 39 A comparison of the chains $\{Z_nR_{4n}\}$ with $n = 1, 3, 5$ as observed (from left to right) in $\{OsSc_4\}Cl_4$, $\{Ir_3Sc_{12}\}Br_{16}$, and $\{Os_5Lu_{20}\}I_{24}$. The repeat units are indicated by red rectangles

15.67 for $\{Ir_3Sc_{12}\}Br_{16}$, and 15.2 for $\{Os_5Lu_{20}\}I_{24}$. This electron count has roughly been seen for many compounds with oligomeric or extended structures of cluster complexes with endohedral transition metal atoms. In this connection, it must be noted that $\{Ru_3Sc_{12}\}Te_8Sc_{2-x}$[117] has, if x were 0, the same number of cluster-based electrons as $\{Ir_3Sc_{12}\}Br_{16}$ and, furthermore the cluster chain structure $\{Z_3Sc_{12}\}$ (Z = Ru, Ir) is the same. This is an important hint at a chemistry in which bromide and telluride ligands could also be partially substituted.

Again, chemical bonding must be considered as predominantly intracluster Z–R bonding and polar R–X bonding. Figure 40 shows crystal orbital overlap populations

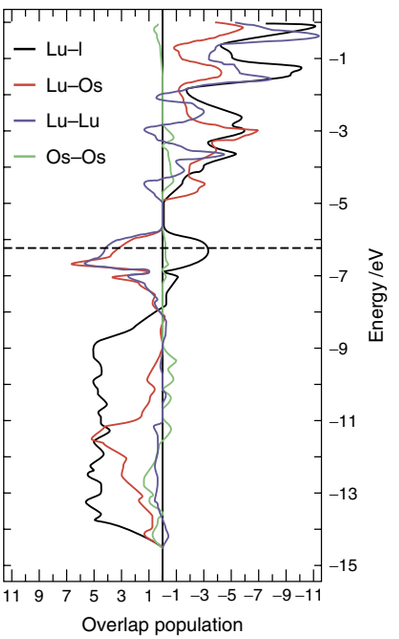

Figure 40 Crystal orbital overlap populations for Lu–I, Lu–Os, Lu–Lu, and Os–Os in $\{Os_5Lu_{20}\}I_{24}$

(COOP) for $\{Os_5Lu_{20}\}I_{24}$. It is the usual pattern: Os–Lu and Lu–I bonding interactions are low in energy, with some Lu–I antibonding close to the Fermi level. It is remarkable that there is considerable Lu–Lu bonding right at the Fermi level, which is not seen with other rare earth elements. This means that there is, although the electronic configuration should be $4f^{14}$, a remarkable contribution of 5d states, and, thus, lutetium could already be considered a transition metal.

6 CONCLUSIONS

Rare earth elements R with high reduction potentials $E°$ (R^{3+}/R^{2+}) originating from low third ionization potentials I_3, i.e., R = La, Ce, Pr, (Nd), Gd, Tb, Dy, Ho, Er, Lu, Y, Sc, are capable of forming clusters $\{R_x\}$. Almost all of the observed clusters contain an endohedral atom Z. The majority of these clusters are octahedral, $\{ZRx_6\}$, but the coordination number of the endohedral atom can also be four, or seven and eight. The clusters are surrounded by halido ligands X; the cluster complexes then have the general composition $\{ZR_x\}X_z$. Isolated cluster complexes are rare. They are usually connected via common ligands and, more importantly, share common cluster atoms building oligomers, chains, and layers. Bonding in cluster complexes is predominantly Z-R and polar R-X bonding with usually only little homoatomic R-R or Z-Z bonding.

7 GLOSSARY

anti-Werner complex: a central metal (or nonmetal) atom with high electron affinity surrounded by unlike metal atoms forming a cluster and further by electronegative ligands

Band structure: *k*-space-dependent energy-level diagram for an extended solid, similar to the molecular orbital diagram at the gamma point

Configuration crossover: transition from one electronic configuration to another

Conproportionation: compounds with higher and lower oxidation states of one element react to a compound with an oxidation state in between

Coordination number (CN): the number of atoms surrounding a central (metal) atom in a coordination complex

Cluster: according to Cotton ''a group of two or more metal atoms in which there are substantial and direct bonds between the metal atoms,'' put in braces {. . .} in this chapter

Cluster complex: a cluster surrounded by ligands, $\{R_x\}X_z$

Crystal orbital Hamiltonian population (COHP): like COOP, different weighting scheme

Crystal orbital orbital population (COOP): from the density of states of band structure calculations, showing the degree of bonding and antibonding interactions between atom types in a solid

Density of states (DOS): number of states per interval of energy at each energy level that are available to be occupied by electrons in a solid

Electronic configuration: energy levels in the shell of an atom that are occupied with electrons; symbolized by quantum numbers

Endohedral atom: atom Z in the center of a cluster, $\{ZR_x\}X_z$

Extended structures: crystal structures with polyhedra connected to a one-, two-, or three-dimensional arrangement

Fermi level: highest occupied energy level in a solid

Interstitial: an atom occupying an interstice; synonymous with endohedral atom

Isolated cluster: a cluster that does not share cluster atoms with other clusters

Lanthanides: the elements La, Ce–Lu

Metallothermic reduction: reduction of a metal oxide or halide with a highly reductive metal

Naked cluster: a cluster of metal atoms that has no ligand sphere

Oligomeric cluster: a cluster that is built from clusters sharing common cluster atoms

Rare earth elements (metals): the elements Sc, Y, La, and the lanthanoids Ce through Lu

Rare earths: oxides of the rare earth elements, in most cases of the composition R_2O_3

Reduced rare earth halides: halides with the rare earth element in an oxidation state less than +3

Supertetrahedron: a tetrahedron built of tetrahedra; the edge length of a supertetrahedron T3, for example, is three times the edge length of the constituting tetrahedron

Valence: according to Pauling (1949) ''the number of other atoms with which an atom of a certain element can combine''

Valence electron(s): electron(s) constituting the valence shell beyond the core (usually a noble gas configuration)

Werner complex: a central metal atom surrounded by ligands

8 RELATED ARTICLES

The Electronic Structure of the Lanthanides; Lanthanides: Coordination Chemistry; The Divalent State in Solid Rare Earth Metal Halides; Lanthanide Halides.

9 ABBREVIATIONS AND ACRONYMS

[. . .]	Square brackets indicate a Werner-type complex
{. . .}	Braces indicate a cluster
A	Alkali metal atom
°C	Degrees Celsius; temperature scale after Celsius
CN	Coordination number
COHP	Crystal orbital Hamiltonian population
COOP	Crystal orbital overlap population
D	Distance (between the nuclei of two atoms)
DOS	Density of states
E°	Standard electrode potential (in V)
EHMO	Extended Hückel molecular orbital (theory)

$\Delta H°$	Enthalpy difference under standard conditions (in kJ mol^{-1})
$\Delta H°(\mathbf{3})$	Third ionization potential (in kJ mol^{-1})
HOMO	Highest occupied molecular orbital
I_3	Third ionization potential (in eV or kJ mol^{-1})
K	Kelvin; absolute temperature scale
LMTO-ASA	The linear muffin tin orbital method implemented in the atomic sphere approximation
LUMO	Lowest unoccupied molecular orbital
MO	Molecular orbital
pm	Picometer, 10^{-12} m
R	Rare earth and lanthanide element (Sc, Y, La, Ce–Lu)
SOMO	Singly occupied molecular orbital
X	Halogen atom, X^- halide ion
[Xe]	Electronic configuration of a xenon atom
V	Volt; unit of voltage
VB	Valence bond (theory)
VE	Valence electron(s)

10 REFERENCES

1. F. A. Cotton and G. Wilkinson, 'Advanced Inorganic Chemistry', Wiley-Interscience, New York, Chichester, Brisbane, Toronto, Singapore, 5th edition, 1988, Chap. 23, p. 1053.
2. P. Niggli, *Z. Anorg. Allg. Chem.*, 1916, **94**, 207.
3. H. Schäfer and H. G. Schnering, *Angew. Chem.*, 1964, **76**, 833.
4. G. Meyer, *Z. Anorg. Allg. Chem.*, 2008, **634**, 2729.
5. P. Niggli, 'Grundlagen der Stereochemie', Birkhäuser, Basel, 1946.
6. D. A. Johnson, *J. Chem. Soc. A*, 1969, 1525, 1529, 2578.
7. L. R. Morss, in 'Standard Potentials in Aqueous Solution', eds. A. J. Bard, R. Parsons, and J. Jordan, Marcel Dekker, New York, 1985, p. 587.
8. G. Meyer, *Chem. Rev.*, 1988, **88**, 93.
9. D. A. Johnson, 'Some Thermodynamic Aspects of Inorganic Chemistry', 2nd edition, Cambridge University Press, Cambridge, 1982.
10. D. A. Johnson, in 'Inorganic Chemistry in Focus', eds. G. Meyer, D. Naumann, and L. Wesemann, Wiley-VCH, Weinheim, 2006, Vol. 3, p. 1.
11. L. R. Morss, *Chem. Rev.*, 1976, **76**, 827.
12. J. D. Corbett, in 'Synthesis of Lanthanide and Actinide Compounds', eds. G. Meyer and L. R. Morss, Kluwer Academic Publishers, Dordrecht, NL, 1991, p. 159.
13. G. Meyer and T. Schleid, in 'Synthesis of Lanthanide and Actinide Compounds', eds. G. Meyer and L. R. Morss, Kluwer Academic Publishers, Dordrecht, NL, 1991, p. 175.
14. G. Meyer, *Z. Anorg. Allg. Chem.*, 2007, **633**, 2537.
15. A. Simon, *Angew. Chem. Int. Ed.*, 1981, **20**, 1.
16. A. Simon, H. J. Mattausch, G. J. Miller, W. Bauhofer, and R. K. Kremer, in 'Handbook on the Physics and Chemistry of Rare Earths', eds. K. A. Gschneidner, Jr. and L. Eyring, North Holland, Amsterdam, 1991, Vol. 15, p. 191.
17. A. Simon, H. Mattausch, and N. Holzer, *Angew. Chem. Int. Ed.*, 1977, **15**, 624.
18. B. C. McCollum, M. J. Camp, and J. D. Corbett, *Inorg. Chem.*, 1973, **12**, 778.
19. J. E. Mee and J. D. Corbett, *Inorg. Chem.*, 1965, **4**, 88.
20. D. A. Lokken and J. D. Corbett, *Inorg. Chem.*, 1973, **12**, 556.
21. A. Simon, N. Holzer, and H. Mattausch, *Z. Anorg. Allg. Chem.*, 1979, **456**, 207.
22. L. R. Morss, H. Mattausch, R. K. Kremer, A. Simon, and J. D. Corbett, *Inorg. Chim. Acta*, 1987, **140**, 107.
23. K. R. Poeppelmeier and J. D. Corbett, *Inorg. Chem.*, 1977, **16**, 1107.
24. J. D. Martin and J. D. Corbett, *Angew. Chem. Int. Ed.*, 1995, **34**, 233.
25. M. Ryazanov, L. Kienle, A. Simon, and H. Mattausch, *Inorg. Chem.*, 2006, **45**, 2068.
26. A. Werner, *Z. Anorg. Chem.*, 1915, **92**, 376.
27. N. Gerlitzki, S. Hammerich, I. Pantenburg, and G. Meyer, *Z. Anorg. Allg. Chem.*, 2006, **632**, 2024.
28. A. Simon and T. Koehler, *J. Less-Common Met.*, 1986, **116**, 279.
29. U. Schwanitz-Schüller and A. Simon, *Z. Naturforsch.*, 1985, **40b**, 705.
30. S. Uhrlandt and G. Meyer, *J. Alloys Compd.*, 1995, **225**, 171.
31. H. Mattfeld and G. Meyer, *Z. Anorg. Allg. Chem.*, 1994, **620**, 85.
32. M. Lulei and J. D. Corbett, *Inorg.Chem.*, 1995, **34**, 2671.
33. U. Beck and A. Simon, *Z. Anorg. Allg. Chem.*, 1997, **623**, 1011.
34. M. C. Schaloske, L. Kienle, C. Hoch, H. Mattausch, R. K. Kremer, and A. Simon, *Z. Anorg. Allg. Chem.*, 2009, **635**, 1023.
35. H. Mattausch, C. Hoch, and A. Simon, *Z. Naturforsch.*, 2007, **62b**, 143.
36. M. C. Schaloske, H. Mattausch, L. Kienle, and A. Simon, *Z. Anorg. Allg. Chem.*, 2008, **634**, 1493.
37. L. Jongen, A.-V. Mudring, and G. Meyer, *Angew. Chem. Int. Ed.*, 2006, **45**, 1886.
38. J. Li, H.-J. Zhai, and L.-S. Wang, *Science*, 2003, **299**, 864.
39. R. B. King, Z. Chen, and P. R. Schleyer, *Inorg. Chem.*, 2004, **43**, 4564.
40. G. Meyer and S. Uhrlandt, *Angew. Chem. Int. Ed.*, 1993, **32**, 1318.
41. S. Uhrlandt and G. Meyer, *Z. Anorg. Allg. Chem.*, 1994, **620**, 1872.

42. S. Uhrlandt, T. Heuer, and G. Meyer, *Z. Anorg. Allg. Chem.*, 1995, **621**, 1299.
43. S. Uhrlandt and G. Meyer, *Z. Anorg. Allg. Chem.*, 1995, **621**, 1466.
44. T. Heuer, F. Steffen, and G. Meyer, *Eur. J. Solid State Inorg. Chem.*, 1996, **33**, 265.
45. H. Mattausch, C. Hoch, and A. Simon, *Z. Anorg. Allg. Chem.*, 2008, **634**, 641.
46. H. Artelt, T. Schleid, and G. Meyer, *Z. Anorg. Allg. Chem.*, 1992, **618**, 18.
47. C. Rustige, M. Brühmann, S. Steinberg, E. Meyer, K. Daub, S. Zimmermann, M. Wolberg, A.-V. Mudring, and G. Meyer, *Z. Anorg. Allg. Chem.*, 2012, **638**.
48. J. D. Corbett, R. L. Daake, K. R. Poeppelmeier, and D. H. Guthrie, *J. Am. Chem. Soc.*, 1978, **100**, 652.
49. T. Hughbanks and J. D. Corbett, *Inorg. Chem.*, 1989, **28**, 631.
50. S.-J. Hwu and J. D. Corbett, *J. Solid State Chem.*, 1986, **64**, 331.
51. K. Daub and G. Meyer, *Acta Crystallogr.*, 2008, **E64**, i4.
52. D. S. Dudis and J. D. Corbett, *Inorg. Chem.*, 1987, **26**, 1933.
53. G. Meyer and M. S. Wickleder, in 'Handbook on the Physics and Chemistry of Rare Earths', eds. K. A. Gschneidner, Jr. and L. Eyring, Elsevier, 2000,, Vol. 28, p. 53.
54. A. Simon, E. Warkentin, and R. Masse, *Angew. Chem. Int. Ed.*, 1981, **20**, 1013.
55. H. M. Artelt and G. Meyer, *Z. Anorg. Allg. Chem.*, 1994, **620**, 1527.
56. H. Mattausch, A. Simon, L. Kienle, C. Hoch, C. Zheng, and R. K. Kremer, *Z. Anorg. Allg. Chem.*, 2006, **632**, 1661.
57. R. Wiglusz and G. Meyer, *Z. Kristallogr., New Cryst. Struct.*, 2007, **222**, 9.
58. M. Brühmann and G. Meyer, *Eur. J. Inorg. Chem.*, 2010, 2609.
59. H. Mattausch, G. V. Vajenine, O. Oeckler, R. K. Kremer, and A. Simon, *Z. Anorg. Allg. Chem.*, 2001, **627**, 2542.
60. M. Brühmann, Cluster-Komplexe der Seltenerdmetalle Gadolinium und Lutetium mit endohedralen Übergangsmetall-Atomen, Dr. rer. nat. Dissertation, Universität zu Köln, 2011.
61. M. W. Payne, M. Ebihara, and J. D. Corbett, *Angew. Chem. Int. Ed. Engl.*, 1991, **30**, 856.
62. M. Ebihara, J. D. Martin, and J. D. Corbett, *Inorg. Chem.*, 1994, **33**, 2079.
63. S. J. Steinwand and J. D. Corbett, *Inorg. Chem.*, 1996, **35**, 7056.
64. S. J. Steinwand, J. D. Corbett, and J. D. Martin, *Inorg. Chem.*, 1997, **36**, 6413.
65. S. Zimmermann, Hochkoordinierte endohedrale Übergangs-metallatome in Scandiumclustern, Dr. rer. nat. Dissertation, Universität zu Köln, 2008.
66. K. Daub, New Interstitially Stabilized Cluster Complexes of Dysprosium, Holmium and Erbium, Dr. rer. nat. Dissertation, Universität zu Köln, 2009.
67. C. Rustige, Interstitiell stabilisierte Clusterkomplexe der Seltenerdmetalle Terbium und Erbium, Dr. rer. nat. Dissertation, Universität zu Köln, 2011.
68. E. Warkentin and H. Bärnighausen, *Z. Anorg. Allg. Chem.*, 1979, **459**, 187.
69. K. Daub and G. Meyer, *Z. Anorg. Allg. Chem.*, 2010, **636**, 1716.
70. C. Zheng, J. Köhler, H. Mattausch, C. Hoch, and A. Simon, *J. Am. Chem. Soc.*, 2012, **134**, 5026.
71. S. Steinberg, Dr. rer. nat. Dissertation, Universität zu Köln, 2013.
72. H. Mattausch and A. Simon, *Z. Kristallogr., New Cryst. Struct.*, 2005, **220**, 313.
73. H. Mattausch, O. Oeckler, and A. Simon, *Z. Kristallogr., New Cryst. Struct.*, 2003, **218**, 282.
74. H. Mattausch, C. Hoch, and A. Simon, *Z. Naturforsch.*, 2007, **62b**, 148.
75. H. Mattausch and A. Simon, *Z. Kristallogr., New Cryst. Struct.*, 1997, **212**, 99.
76. H. Mattausch, O. Oeckler, and A. Simon, *Z. Kristallogr., New Cryst. Struct.*, 2000, **215**, 199.
77. M. Lukachuk, H. Mattausch, and A. Simon, *Z. Kristallogr., New Cryst. Struct.*, 2006, **221**, 3.
78. K. R. Poeppelmeier and J. D. Corbett, *J. Am. Chem. Soc.*, 1978, **100**, 5039.
79. S. M. Kauzlarich, T. Hughbanks, J. D. Corbett, P. Klavins, and R. N. Shelton, *Inorg. Chem.*, 1988, **27**, 1791.
80. A. Nagaki, A. Simon, and H. Borrmann, *J. Less-Common Met.*, 1989, **156**, 193.
81. H. Mattausch, M. C. Schaloske, C. Hoch, Ch. Zheng, and A. Simon, *Z. Anorg. Allg. Chem.*, 2008, **634**, 491.
82. H. Mattausch, M. C. Schaloske, C. Hoch, and A. Simon, *Z. Anorg. Allg. Chem.*, 2008, **634**, 498.
83. H. Mattausch, O. Oeckler, and A. Simon, *Z. Anorg. Allg. Chem.*, 2008, **634**, 503.
84. H. Mattausch, A. Simon, and R. Eger, *Rev. Chim. Miner.*, 1980, **17**, 516.
85. S.-J. Hwu, D. S. Dudis, and J. D. Corbett, *Inorg. Chem.*, 1987, **26**, 469.
86. A. Simon and E. Warkentin, *Z. Anorg. Allg. Chem.*, 1983, **497**, 79.
87. S. Uhrlandt and G. Meyer, *Z. Kristallogr., New Cryst. Struct.*, 1995, **210**, 361.
88. M. Ryazanov, H. Mattausch, and A. Simon, *J. Solid State Chem.*, 2007, **180**, 1372.
89. E. Warkentin and A. Simon, *Rev. Chim. Miner.*, 1983, **20**, 488.
90. C. Zheng, O. Oeckler, H. Mattausch, and A. Simon, *Z. Anorg. Allg. Chem.*, 2001, **627**, 2151.
91. M. W. Payne, P. K. Dorhout, S.-J. Kim, T. R. Hughbanks, and J. D. Corbett, *Inorg. Chem.*, 1992, **31**, 1389.
92. R. Llusar and J. D. Corbett, *Inorg. Chem.*, 1994, **33**, 849.

93. N. Herzmann, A.-V. Mudring, and G. Meyer, *Inorg. Chem.*, 2008, **47**, 7954.
94. S. Gupta, G. Meyer, and J. D. Corbett, *Inorg. Chem.*, 2010, **49**, 9949.
95. S.-J. Hwu, J. D. Corbett, and K. R. Poeppelmeier, *J. Solid State Chem.*, 1985, **57**, 43.
96. S. Zimmermann, Hochkoordinierte endohedrale Übergangs-metallatome in Scandiumclustern, Dr. rer. nat. Dissertation, Universität zu Köln, 2008.
97 K. Berroth, Dr. rer. nat. Dissertation, Universität Stuttgart, 1980.
98. K. Berroth, H. Mattausch, and A. Simon, *Z. Naturforsch.*, 1980, **35b**, 626.
99. A. Simon, *J. Solid State Chem.*, 1985, **57**, 2.
100. H. Mattausch, W. Schramm, W. Eger, A. Simon, *Z. Anorg. Allg. Chem.*, 1985, **530**, 43.
101. D. G. Adolphson and J. D. Corbett, *Inorg. Chem.*, 1976, **15**, 1820.
102. R. L. Daake and J. D. Corbett, *Inorg. Chem.*, 1977, **16**, 2029.
103. G. Meyer, S.-J. Hwu, S. Wijeyesekera, and J. D. Corbett, *Inorg. Chem.*, 1986, **25**, 4811.
104. U. Schwanitz-Schüller and A. Simon, *Z. Naturforsch.*, 1985, **40b**, 710.
105. T. Schleid and G. Meyer, *Z. Anorg. Allg. Chem.*, 1987, **552**, 90.
106. A. Palasyuk, I. Pantenburg, and G. Meyer, *Z. Anorg. Allg. Chem.*, 2006, **632**, 1969.
107. M. Ruck and A. Simon, *Z. Anorg. Allg. Chem.*, 1993, **619**, 327.
108. Y. Park, J. D. Martin, and J. D. Corbett, *J. Solid State Chem.*, 1997, **129**, 277.
109. C. Lefevre, C. Hoch, R. K. Kremer, and A. Simon, *Solid State Sci.*, 2008, **10**, 1625.
110. H. Mattausch, C. Schwarz, and A. Simon, *Z. Kristallogr.*, 1987, **178**, 156.
111. A. Simon, C. Schwarz, and W. Bauhofer, *J. Less-Common Met.*, 1988, **137**, 343.
112. H. Mattausch, H. Borrmann, and A. Simon, *Z. Naturforsch.*, 1993, **48b**, 1828.
113. H. Mattfeld, K. Krämer, and G. Meyer, *Z. Anorg. Allg. Chem.*, 1993, **619**, 1384.
114. P. K. Dorhout and J. D. Corbett, *J. Am. Chem. Soc.*, 1992, **114**, 1697.
115. S. Zimmermann, M. Brühmann, F. Casper, O. Heyer, T. Lorenz, C. Felser, A.-V. Mudring, and G. Meyer, *Eur. J. Inorg. Chem.*, 2010, 2613.
116. M. Brühmann, A.-V. Mudring, M. Valldor, and G. Meyer, *Eur. J. Inorg. Chem.*, 2012, 4083.
117. L. Chen and J. D. Corbett, *J. Am. Chem. Soc.*, 2003, **125**, 1170.